

Influence of soil moisture initial conditions in a Regional Climate Model study over West Africa: Part 1: Impact on the climate mean.

Brahima KONÉ¹, Arona DIEDHIOU^{1, 2}, Adama Diawara¹, Sandrine Anquetin², N'datchoh Evelyne Touré¹, Adama Bamba¹, and Arsene Toka Koba¹

¹LAPAMF, Université Félix Houphouët Boigny, Abidjan, Côte d'Ivoire

²Univ. Grenoble Alpes, IRD, CNRS, Grenoble INP, IGE, F-38000 Grenoble, France

Correspondence to: Arona DIEDHIOU (aronadiedhiou@ird.fr)

Abstract.

The impact of soil moisture initial conditions on the mean climate over West Africa is examined using the latest version of the Regional Climate Model of the International Centre for Theoretical Physics (RegCM4) at the horizontal resolution of 25 km × 25 km. We performed these sensitivity studies to the initial conditions of soil moisture for June-July-August-September (JJAS) from 2001 to 2005 with a focus on two contrasted years 2003 (above normal precipitation year) and 2004 (below normal precipitation year). The soil moisture reanalysis of the European Centre Meteorological Weather Forecast's reanalysis of the 20th century (ERA20C) were used to initialize the control runs, whereas we initialized the soil moisture at the wilting points and field capacity with dry and wet soil moisture initial conditions respectively (hereafter dry and wet experiments). The impact of soil moisture initial condition on the precipitation in West Africa is homogeneous only over the Central Sahel where dry (wet) experiment lead to rainfall decrease (increase). The strongest impact on precipitation in wet experiments is found over the West Sahel with the peak of change about respectively +40%, while the strongest decrease is found in dry experiments over Central Sahel with a peak of change about -8%. The sensitivity of soil moisture initial condition can persist for three to four months (90-120 days) depending on the region. However, the influence on precipitation is no longer than one month (between 15days and 30 days). Overall, the impact of soil moisture initial conditions is greater on temperature than on precipitation. The strongest impact is located over the Central Sahel with the peak of change of -1.5 °C and 0.5°C respectively in wet and dry experiments. Mechanisms associated with the influence of soil moisture initial conditions on mean precipitation and temperature are highlighted. In the Part II of this study, the influence of the soil moisture initial conditions on climate extremes is investigated.

33 **1 Introduction**

34 In the climate system, soil moisture is one of the crucial variables which influence water balance
35 and surface energy components through latent surface fluxes and evaporation. Therefore, soil
36 moisture impacts the development of weather patterns and precipitation production. The strength
37 of soil moisture impact on land-atmosphere coupling is variable according to the place and with
38 the season. Koster et al. (2004) sustained that the atmospheric response simulation to the slow
39 variation of the ocean and land surface states, can accurate the seasonal simulations. The
40 atmosphere response to ocean temperature anomalies is well documented (Kirtman et al. 1998;
41 Rasmusson et al.1982). Another earth system component, potentially useful, that varies slowly is
42 soil moisture. The role of the soils may be comparable to that of the oceans. While in summer, the
43 solar energy received by the oceans is stored (and use it to heat the atmosphere in winter), in winter
44 the precipitation received by the soil is stored (the moistening and cooling is returned to the
45 atmosphere in summer). Through its impact on surface energy fluxes and evaporation, there are
46 many additional impacts on climate process of soil moisture, such as boundary-layer stability and
47 air temperature (Hong and Pan, 2000; Kim and Hong 2006). Several studies have shown that the
48 anomalies of the soil moisture may persist for several weeks or months, however, its impact
49 remains only for a shorter time in the atmosphere, not exceed few days (Vinnikov and Yeserkepova
50 1991; Liu et al., 2014). The important role of the anomalies in soil moisture in the coupling of land
51 and atmosphere is shown in several studies, using numerical climate models (Jaeger et al., 2011;
52 Zhang et al., 2011) and observation datasets (Zhang et al., 2008a; Dirmeyer et al., 2006).

53 West Africa is known to be a region where there is a strong coupling between soil moisture and
54 precipitation (Koster et al., 2004). Several previous studies have been conducted over West Africa
55 on a global scale using AGCMs (Atmospheric General Circulation Model) to investigate the
56 impact on the land-atmosphere coupling of soil moisture anomalies (Koster et al., 2004; Douville
57 and al, 2001; Zhang et al., 2008b). However, at the local and regional scales, the land-atmosphere
58 coupling studies with AGCM, present large uncertainties (Xue et al. 2010). Recently, the use of
59 RCMs to simulate the impact on interannual climate variability of anomalies in soil moisture
60 received a lot of attention because of the increase in climate variability associated with extreme
61 weather events that can have greater societal and environmental impacts. In general, these studies
62 have been conducted for Asia, Europe and America (e.g. Seneviratne et al. 2006 for Europe; Zhang
63 et al. 2011 for Asia; Zhang et al. 2008b for America). Overall, the results of these studies show,
64 during summertime, the strong impact of the anomalies of soil moisture in land-atmosphere
65 occurred mainly over the transition zones with a climate between wet and dry climate regimes.
66 The relevance and extent of this potential feedback are still poorly understood over West Africa.

67 This study will focus on the influence of soil moisture initial conditions anomalies on climate mean
68 and it is based on performance assessment of the Regional Climate model version 4 coupled to the
69 version 4.5 of the Community Land Model (RegCM4-CLM4.5) done by Koné et al. (2018) where
70 the ability of the model to reproduce the climate mean has been validated. This study will help us
71 to understand the impacts of Soil Moisture Initial Conditions on the new dynamical core non-
72 hydrostatic of RegCM4 in the context of land-atmosphere coupling. We attempt, also, in this study
73 to provide the quantification of the sensitivity of the RegCM4 model to initial soil moisture
74 conditions, which could allow the evaluation and development of the RegCM4 model. However,
75 in the part II of the article, the influence of soil moisture on climate extremes will be explored. The
76 descriptions of the model and experiment setup used in this study are presented in Section. 2; in
77 the Section 3, the influence of the anomalies in soil moisture initial conditions on the subsequent
78 climate mean is analyzed and discussed; and in Section 4 the main conclusions close the paper.

79 **2. Model and experimental design**

80 **2.1 Descriptions of the model and the observed datasets**

81 We used in this study, the fourth generation of the Regional Climate Model (RegCM4) of the
82 International Centre for Theoretical Physics (ICTP). Since this release, the physical
83 representations have been submitted to a continuous process of development and
84 implementation. The version used in the present study is RegCM4.7. The MM5 (Grell et al.,
85 1994) non-hydrostatic dynamical core has been ported to RegCM without removing the existing
86 hydrostatic core. The model dynamical core used in this study is non-hydrostatic. RegCM4 is
87 a limited area model using a sigma pressure vertical grid and the finite differencing algorithm
88 of Arakawa B-grid (Giorgi et al., 2012). The radiation scheme used in this version of RegCM4.7
89 is derived from NCAR (National Center for Atmospheric Research) Community Climate Model
90 Version 3 (CCM3) (Kiehl et al., 1996), the representation of aerosols is from Zakey et al. (2006)
91 and Solmon et al. (2006). The scheme of the large-scale precipitation used is from Pal et al.
92 (2000), the moisture scheme is the SUBEX (SUBgrid EXplicit moisture scheme) takes in
93 account the cloud variability scale sub-grid, and the accretion processes and evaporation for
94 stable precipitation following the work of Sundqvist et al., 1989. In the planetary boundary
95 layer, the sensible heat over ocean and land, the water vapour and the turbulent transports of
96 momentum are calculated according to the scheme of Holtslag et al. (1990). The heat and
97 moisture, the momentum fluxes of ocean surfaces in this study are computed as in Zeng et al.
98 (1998). In RegCM4.7, convective precipitation and the land surface processes can be described
99 by several parameterizations. Based on Koné et al. (2018), we selected the convective scheme

100 of Emanuel (Emanuel, 1991) and the interaction processes between soil, vegetation and
101 atmosphere are parameterized with CLM4.5. In each grid cell, CLM4.5 has 16 different PFTs
102 (Plant Functional Types) and 10 soil layers (Lawrence et al., 2011; Wang et al., 2016). RegCM4
103 was integrated over the domain of West Africa depicted in Fig. 1 with 25 km (182x114 grid
104 points; from 20°W-20°E and 5°S-21°N) of horizontal resolution and with 18 vertical levels and
105 the initial and boundary conditions are from the European Centre for Medium-Range Weather
106 Forecasts reanalysis (EIN75; Uppala et al., 2008; Simmons et al., 2007). The Sea Surface
107 Temperatures (SST) is from the National Oceanic and Atmosphere Administration (NOAA)
108 optimal interpolation weekly (OI_WK) (Reynolds et al., 1996). The source for the topography
109 is from States Geological Survey (USGS) Global Multi-resolution Terrain Elevation Data
110 (GMTED; Danielson et al., 2011) at 30 arc-second spatial resolution which is an update to the
111 Global Land Cover Characterization (GTOPO; Loveland et al., 2000) dataset.

112 Our analysis is focused on the precipitation and the 2m air temperature over the West African
113 domain during the summer of June-July-August-September (JJAS) for 2003 and 2004. The
114 uncertainties reduction related to the absence of reliable observation system over the region (Sylla
115 et al., 2013a; Nikulin et al., 2012), we validated the simulated precipitation based on two products:
116 the TRMM datasets (Tropical Rainfall Measuring Mission 3B43V7) at the high-resolution 0.25°,
117 available from 1998 to 2013 (Huffman et al., 2007), and The Climate Hazards Group Infrared
118 Precipitation with Stations (CHIRPS) dataset developed at the University of California at Santa
119 Barbara at the 0.05° high-resolution available from 1981 to 2020. The validation of the simulated
120 2 m temperature relies on two observational datasets: the global daily temperature from the Global
121 Telecommunication System (hereafter GTS), gridded at 0.5° of horizontal resolution for 1979 to
122 2020 (Fan and van den Dool, 2008) and the CRU datasets (Climate Research Unit version 3.20)
123 from the University of East Anglia, gridded at the horizontal resolution 0.5° and available from
124 1901 to 2011 (Harris et al., 2013). To facilitate the comparison with RegCM4 simulations, all
125 products are re-gridded to 0.22° × 0.22° using a method of bilinear interpolation (Nikulin et al.,
126 2012).

127

128 **2.2 Experiments setup and analysis methodology**

129 We set up an ensemble of 3 experiments each with simulations starting from June 1st to September
130 30th. The difference between these 3 experiments is on the change of soil moisture initial condition
131 during the first day of the simulation (June 1st): For each experiment, we applied (i) a reference

132 initial soil moisture condition, (ii) then a wet initial soil moisture condition, and finally (iii) a dry
133 initial soil moisture condition.

134 We run the simulations over 5 years (2001 to 2005) during the months of June to September over
135 our West African domain. We choose two extreme years (resp. the wettest and the driest year)
136 among the 5 years to observe the estimates of the limits of the impact of internal soil moisture
137 forcing on the new dynamical core non-hydrostatic of RegCM4. It is in the same context, several
138 previous studies chosen two extreme years for their sensitivity study of initial soil moisture
139 condition on the models. Hong and al. (2000) use in their study only two years (3 months per year)
140 to investigate the impact of initial soil moisture over the North of America (in the Great Plains)
141 during the two summers, May-June-July (MJJ) 1988 (corresponding to a drought in the Great
142 plains) and MJJ 1993 (correspond to a flooding event). Over Asia, Kim and Hong (2006) used two
143 contrasted years 1997 (below normal precipitation year) and 1998 (above normal precipitation
144 year). The first 7 days (Kang et al., 2014) are excluded in the analysis as a spin-up period.

145 With very little variation in soil moisture in one day, soil moisture initial conditions are given at
146 the first step of June 1st for the two summers JJAS 2003 and JJAS 2004. Except for the
147 geographical location, the experimental setup is the same as that of Hong and Pan (2000). The
148 geographical location of this study is the same as in Koné et al (2018), with four sub-regions (Fig.
149 1), each with different features of the annual cycle of precipitation: Central Sahel (10°W–10°E;
150 10°N-16°N), West Sahel (18°W-10°W; 10°N-16°N), and Guinea Coast (15°W-10°E; 3°N-10°N).
151 For each year, three experiments are conducted; we used the soil moisture from the reanalysis of
152 the European Centre Meteorological Weather Forecast's reanalysis of the 20th century (ERA20C)
153 to initialize the control runs. We initialized the dry and wet soil moisture initial conditions (in
154 volumetric fraction $\text{m}^3.\text{m}^{-3}$) respectively at the wilting point ($=0.117*10^{-4}$) and the field capacity
155 ($=0.489$) derived from ERA20C dataset. The wilting point and the field capacity correspond to the
156 minimum and maximum values of soil moisture over our studied simulation studied.

157 Generally, in several previous studies (Liu et al. (2014), Hong and Pan (2000), Kim and Hong
158 (2006)), the analysis methodology used is the mean biases (MB) averaged over their domains
159 studied to quantify the impact of soil moisture anomalies, while in our study we used the mean
160 biases and the probability density function (PDF, Gao et al. 2016; Jaeger and Seneviratne 2011)
161 by fitting a normal distribution for this purpose to better capture how many grid points are
162 impacted by the soil moisture initial conditions. The pattern correlation coefficient (PCC) is also
163 used as a spatial correlation to reveal the degree of large-scale similarity between model
164 simulations and the observation. We used the two-tailed of the student's t-distribution to
165 investigate the differences which are statistically significant at each grid cell between the control

166 and the sensitivity experiments (wet and dry). For the regional analysis such as MB, PCC and the
167 PDF, both modeled and observed temperature and precipitation values were calculated only over
168 land grid points.

169

170 3. Results and discussion

171 3.1. Influence of soil moisture initial conditions on precipitation.

172 In the aim to identify the extreme years (driest and wettest) impacted by the dry and wet
173 experiments among the five years simulations (2001 to 2005), we display Changes in daily soil
174 moisture for 5 years (2001 to 2005) and their climatological mean during JJAS over West African
175 domain, from dry and wet experiments with respect to their corresponding control experiment in
176 Figure 2. The Fig.2 shows that the weakest and strongest impact of the dry experiments is found
177 for 2003 and 2004 respectively. For a wet year, the impact of drying out soil moisture is quickly
178 erased. While for a dry year the impact of the drying of the soil is accentuated. This meaning that
179 2003 and 2004 are respectively the wettest and driest years in dry experiment. However, for the
180 wet experiments, the weakest impact is found for 2004, and the strongest impact is found for the
181 years 2001, 2002 and 2004. In a dry year, the impact of soil humidification is very quickly erased,
182 while in a wet year the impact of soil humidification is accentuated. The wet experiments confirm
183 the result obtained in dry experiments, 2003 and 2004 are wettest and driest years respectively. To
184 conduct our analyzing to estimate the limits of the impact of internal soil moisture forcing on the
185 new dynamical core non-hydrostatic of RegCM4, we have been used the two extreme years 2003
186 and 2004 (resp. the wettest and the driest years) among the 5 years. Figure 3 displays the spatial
187 distribution of observed mean rainfall (mm/day) from CHIRPS (Fig.3a, d) and TRMM (Fig.3b, e)
188 for JJAS 2003 and JJAS 2004 and their corresponding simulated from control experiments
189 (Fig.3c, f) initialized with reanalysis soil moisture ERA20C. Table 1 reports the MB and the PCC
190 for the simulations of the model and TRMM observation compared to CHIRPS, computed for the
191 central Sahel, Guinea coast, west Sahel and the entire West African domain. CHIRPS product
192 displays a zonal band of rainfall centered around 10° N decreasing from north to south (Fig.3a, d).
193 The maximum values are located over the mountain regions of Cameroun and Guinea. The TRMM
194 observation (Fig.3b, e) is closer to CHIRPS, and represents quite similarly the North–South
195 gradient of precipitation with PCC up to 0.97 over the entire West African domain for both JJAS
196 2003 and JJAS 2004 (Table 1). However, although the observation datasets have similar large-
197 scale patterns, they present differences at the local scale. CHIRPS shows a much larger extend of
198 these maxima than TRMM, especially over the Guinea highland and Cameroon mountains, while

199 TRMM shows a large band of precipitation which extends too far into the Sahel region. The
200 strongest mean biases between the two products are dry about -15.45 % and -16.96 % respectively
201 for JJAS 2003 and JJAS 2004, and are located over the Guinea coast sub-region (Table 1). The
202 control experiments (Fig.3 c and f) initialized with the reanalyze ERA20C soil moisture well
203 reproduce the large-scale pattern of the observed rainfall with PCC 0.72 and 0.77 (Table 1)
204 respectively for JJAS 2003 and JJAS 2004 over the West Africa domain, despite some biases at
205 the locale scale. The spatial extent of rainfall maxima and the North-South gradient are well
206 captured by control experiments; however, their magnitudes are underestimated. In general, the
207 dry mean biases about -49.31% and -50.56% are found respectively for JJAS 2003 and JJAS 2004
208 over the whole West African domain (Table 1). Figure 4 displays change in mean precipitation (in
209 %) for JJAS 2003 and JJAS 2004, for dry and wet experiments with respect to their corresponding
210 control experiments, the dotted area shows changes with statistical significance of 0.05 level.

211 Dry and wet sensitivity experiments show that precipitation has been significantly affected by soil
212 moisture anomalies at varying degrees according to the sub-regions (Fig. 4). For the dry
213 experiments (Fig.4a, c), we found a dominant decrease of rainfall over the central Sahel especially
214 in JJAS 2003 (Fig.4a), while the extent of this decrease is smaller in JJAS 2004(Fig.4c) and
215 confined over the southern-west of Mali. On the other hand, we found a dominant increase of
216 rainfall over the Guinea coast and the west Sahel, although there is a sparse decrease, especially
217 over the Guinea coast. For the wet experiments (Fig.4b, d), there is a dominant increase of rainfall
218 over most of the domains studied with a sparse decrease especially along the coastline of Liberia,
219 Sierra Leone and Guinea for both JJAS 2003 and JJAS 2004 (rep. Fig.4a and c). Overall, the
220 impact on the precipitation of the soil moisture initial conditions is homogeneous particularly over
221 the central Sahel, i.e, the dry (wet) experiments with respect to the control exhibits significant
222 decrease (increase) of precipitations (Fig.4a, b).

223 For a better quantitative evaluation, the PDF distributions of the changes in precipitation in JJAS
224 2003 and JJAS 2004, over (a) central Sahel, (b) West Sahel, (c) Guinea coast and (d) West Africa
225 derived from dry and wet experiments compared to the corresponding control experiments are
226 shown in Figure 5. The impact on the precipitation of soil moisture initial conditions is not
227 homogeneous over most of the studied domains (Fig.5 b-d) except the central Sahel where the dry
228 (wet) experiments with respect to the control display significant decrease (increase) of
229 precipitation (Fig.5a,). However, the strongest impacts on precipitation in wet and dry experiments
230 are found respectively over west and central Sahel, and the peak mode of change are about
231 respectively 40% and -8%. The impacts on precipitation from wet experiments are greater than
232 from dry experiments.

233 It is worth to note that, over the West Sahel and Guinea coast, for both dry and wet experiments
234 tend to cause an increase of precipitation. This indicates that the increased precipitation is likely
235 to occur not only for wet experiments but also for dry experiment (Fig. 5b). The lag between the
236 JJAS 2003 and JJAS 2004 PDFs for wet and dry experiments indicates a somewhat significant
237 impact if we compare the two years, this in particular over Guinea and west Sahel (Fig. 5 b and c).
238 The wet year has a greater impact compared to the dry year in most of domains studied (Fig. 5).
239 These results are consistent with previous studies which supported a strong relationship between
240 precipitation and soil moisture in particular over the transition zones with a climate between wet
241 and dry climate regimes (Koster et al., 2004; Liu et al., 2014; Douville et al., 2001).

242 To better study the influence of soil moisture anomalies on precipitation for the both dry and wet
243 years over the West African domain and its sub-regions, we analyzed changes in the daily domain-
244 average of soil moisture and precipitation (resp. Figure 6 and Figure 7) for JJAS 2003 and JJAS
245 2004, from dry and wet experiments with respect to their corresponding controls experiments. The
246 second soil layer in CLM4.5 (0 to 2.80 cm) is used in this study, this soil layer corresponds to the
247 top layer soil moisture. In general, soil moisture anomalies persist for three or four months over
248 the domains studied (Fig.6). The anomalies of soil moisture disappear for dry and wet experiments
249 with varying duration, between three to four months from one region to another over the domain
250 studied. The strongest duration and amplitude is found over the west Sahel sub-region, for the both
251 wet and dry experiments, it lasts four months in JJAS 2003 and JJAS 2004, although the signal is
252 rather weak in the wet experiments as compared to the dry ones (Fig. 6b). The weaker change in
253 soil moisture anomalies is found over the Guinea coast for wet experiments and lasts three months
254 (Fig. 6c). While in dry experiments, the weaker change in soil moisture anomalies is found over
255 central Sahel and last three months (Fig.6a).

256 Figure 7 shows response of the daily precipitation to the soil moisture initial conditions over the
257 different domains studied. In general, the impact of the wet soil moisture anomalies on daily
258 precipitation is larger in magnitude than that of dry anomalies over most of the domains studied
259 (Fig. 7). The strongest daily precipitation response in dry experiment ($-4\text{mm}\cdot\text{day}^{-1}$) is found over
260 the Guinea coast in the wet year JJAS 2003 (Fig. 7c), while for the wet experiments (more than
261 $8\text{mm}\cdot\text{day}^{-1}$, especially in JJAS 2003), it is found over the West Sahel and the Guinea coast (resp.
262 Fig. 7 b and c). However, the impact on daily precipitation of the soil moisture initial conditions
263 has a much shorter-lived than soil moisture change. The significant impact on daily precipitation,
264 greater than $1\text{mm}\cdot\text{day}^{-1}$ is only shown in wet experiments, and does not last more than fifteen days
265 for most of the domains studied, except for the Guinea coast where it lasts about 1 month. It is
266 worth to note the peaks in precipitation over West Sahel and Guinea coast (resp. Fig.7b and c)

267 during the two months August and September that coincide with fluctuation in the anomalies of
268 soil moisture (Fig.6b and c). This indicates the soil moisture and precipitation feedback is strong
269 during this period over the Guinea coast and West Sahel regions. The response of the daily
270 precipitation to the anomalies in soil moisture initial conditions is also sensitive to the wet and dry
271 year. This is indicated by the lag between dry and wet experiments for JJAS 2003 and JJAS 2004
272 years (Fig7). The magnitude of impacts due to contrasting years depends on the location. For
273 example, over Guinea coast, in the dry experiments, the wet year presents a greater impact
274 compared to the dry year (Fig.7 c). This trend is reversed for the central Sahel (Fig. 7a). These
275 results are in line with the previous works which argued that the soil moisture-atmosphere
276 feedback strength and the land memory depend on the place (Vinnikov et al. 1996; Vinnikov and
277 Yeserkepova 1991).

278 Figure 8 and 9 show the vertical profile change respectively in humidity and temperature for JJAS
279 2003 and JJAS 2004 from the dry and wet experiments with respect to control experiments over
280 the whole West Africa domain and its sub-region indicated in Fig. 1.

281 For the dry and wet experiments, the impact on humidity and temperature (Fig.8 and Fig.9) are
282 significant in the lower troposphere. The dry (wet) soil moisture experiments, in the lower and
283 somewhat in the middle troposphere, show drying (moistening) for humidity and warming
284 (cooling) for temperature. This indicates for dry (wet) experiments a weak (strong) dry convection
285 over most of the domains studied (Fig.8 and Fig.9). The strongest impact on humidity and
286 temperature in lower and middle troposphere is found over central Sahel (Fig.8a and Fig. 9a).
287 These results in the lower troposphere are consistent with the precipitation sensitivity, especially
288 over the central Sahel in JJAS 2003 (Fig.4 a, b). However, over the west Sahel and the Guinea
289 coast this impact is somewhat low compared to that of central Sahel. In the dry experiments over
290 the Guinea coast (Fig.8c), these trends are reversed above 500 hPa for humidity, indicating wet
291 convection in this sub-region. These results in the lower atmosphere are consistent with the
292 precipitation sensitivity over the Guinea coast (Fig.4a, c).

293 On the over hand, in the upper troposphere, the significant impact on humidity and temperature is
294 found only for wet experiments, and exhibits a drying and warming respectively for humidity and
295 temperature over most of the domains studied (Fig.8 and Fig.9). In the wet experiments, the impact
296 on upper tropospheric variability of the anomalies in soil moisture initial conditions is also
297 identified by Hong and Pal (2000). The effect of soil moisture anomalies is mostly confined to the
298 near-surface and somewhat in the upper troposphere. Furthermore, in the upper troposphere,
299 relative humidity responses to the anomalies in soil moisture initial conditions are more sensitive

300 at atmospheric temperature to the contrast of the year, especially, in wet experiments (Fig. 8 and
301 Fig. 9).

302 To understand the origins of the precipitation changes in Figure 4, we analyzed the lower
303 tropospheric wind (850hpa) and moisture changes for JJAS 2003 and JJAS 2004 from the dry and
304 wet experiments with respect to their corresponding control experiments in Figure 10. In the dry
305 experiments, we found a dominant decrease of moistening over most of domain studied, however
306 the strong wind magnitude change over the Atlantic ocean, tends to bring the increase of
307 moistening from the ocean to Guinea coast and west Sahel, this can explain the increase of
308 precipitation over these sub-region in the dry experiments. While over the central Sahel, a weak
309 change in wind magnitude is found, leading to the strong decrease of precipitation there, especially
310 in JJAS 2003 (Fig.4a). On the other hand, for the wet experiments, an increase in moistening is
311 located over most of domain studied. And the strong change in wind magnitude, tend to shift the
312 moistening from the North to the South, leading to increased precipitation over most of domain
313 studied in wet experiments (Fig.4 b and d). These results are broadly consistent to the dry and wet
314 precipitation changes shown in Figure 4.

315 Summarizing this section results, the anomalies in soil moisture anomalies persist for three or four
316 months, while the significant impact on precipitation, greater than $1\text{mm}\cdot\text{day}^{-1}$, of the anomalies in
317 soil moisture is much shorter, no longer than one month. The anomalies in soil moisture initial
318 conditions effect are mostly confined to the near-surface climate and somewhat in the upper
319 troposphere.

320 **3.2. Influence on temperature and other surface fluxes.**

321 The spatial distribution of averaged temperature ($^{\circ}\text{C}$) from CRU (Fig.11 a and d) and GTS (Fig.11
322 b and e) observations for JJAS 2003 and JJAS 2004 and their corresponding simulated from control
323 experiments (Fig.11 c and f) initialized with reanalysis soil moisture ERA20C are shown in Fig.10.
324 Table 2 resumes the PCC and the MB between the simulation of the temperatures and CRU
325 observation, calculated for the west Sahel, central Sahel, Guinea coast and the whole West African
326 domain.

327 The CRU temperature displays a zonal distribution over the whole West Africa domain. Maximum
328 values around 34°C are located over the Sahara, and the lowest temperatures are found on the
329 Guinea coast especially in orographic regions such as Guinean highlands, Cameroon mountains
330 and the Jos Plateau, where the temperature does not exceed 26°C . The two observation datasets
331 GTS and CRU are similar at large spatial scale with PCC about 0.99 over the entire West African
332 domain for both JJAS 2003 and JJAS 2004 (Table 2). However, the extension and the amplitude

333 of these maxima and minima are quite different in the two sets of gridded observations. While
334 GTS (Fig.11b and e) observation displays large (small) areas with maxima (minima) values, CRU
335 (Fig.11a and d) presents small (large) area of these maxima (minima) values. The strongest mean
336 warm biases between the two observation products, about 0.54°C and 0.67°C respectively for JJAS
337 2003 and JJAS 2004, are located over the west Sahel sub-region compared to the others (Table 2).
338 The control experiments (Fig.11 c and f) show a good agreement in the representation of the large-
339 scale pattern of the observed temperature (CRU) with PCC 0.99 for both JJAS 2003 and JJAS
340 2004 (Table 2), including the zone of the meridional gradient of the surface temperature between
341 Sahara Desert and Guinea coast which is crucial for the African easterly jet (AEJ) evolution and
342 formation (Thorncroft and Blackburn 1999; Cook 1999). However, some biases are noted at the
343 local scale. The spatial extent of temperature maxima and minima are well reproduced by control
344 experiments, however their magnitude are overestimate. The strongest warm mean biases of
345 control experiments with respect to CRU observation are about 2.68 °C and 2.14 °C respectively
346 for JJAS 2003 and JJAS 2004, are found over the West Sahel sub-region (Table 2).
347 Figure 12 shows changes in mean temperature (°C) for JJAS 2003 and JJAS 2004, from dry and
348 wet experiments with respect to their corresponding control experiments. The dotted area shows
349 changes that are statistically significant at the 0.05 level. In the dry experiments, for both JJAS
350 2003 and JJAS 2004, the dominant warm changes are located over most of the area under the
351 latitude 13°N, with maximum values located over the Guinea coast. However, a mixture of warm
352 and cool changes is located around the latitude 13°N (Fig.12a and c). On the other hand, for the
353 wet experiments, we found a dominant cool change over most of the area under the latitude 15°N,
354 with maximum values around the latitude 13°N. Whereas a dominant warm change is located
355 above the latitude 15°N (Fig.12 b and d). Overall, the temperature is more sensitive to soil moisture
356 anomalies than precipitation over most of the domains studied.

357 For a better quantitative evaluation, the PDF distributions of the changes in mean temperature in
358 JJAS 2003 and JJAS 2004, over (a) the central Sahel, (b) West Sahel, (c) Guinea and (d) West
359 Africa derived from dry and wet experiments with respect to their corresponding control
360 experiments are shown in Figure 13. The temperature impact is homogeneous over the central
361 Sahel and Guinea coast (Fig.13a and c). The strongest homogeneous impacts on temperature of
362 soil moisture initial conditions anomalies are located over the central Sahel, i.e, the dry (wet)
363 experiments display a decrease (an increase) in temperature change with the peak mode of change
364 at -1.5 °C (0.5°C) compared to other sub-regions, for both JJAS 2003 and JJAS 2004. Over the
365 west Sahel, both wet and dry experiments lead to a decrease of temperature. The impact on
366 temperature of the anomalies in soil moisture is somewhat sensitive to the wet and dry year, as

367 mentioned above, this is indicated by the lag between wet and dry experiments (Fig. 13). The
368 impact on dry and wet years depends on the area and the type of experience dry or wet. Overall,
369 the dry (wet) sensitivity experiments for 2m-temperature show a dominant increase (decrease) of
370 warming (cooling) for both JJAS 2003 and JJAS 2004 over most of the domains studied except
371 for the west Sahel, where both dry and wet experiments lead to an increase of temperature (Fig.13).
372 We now analyze the influence of soil moisture initial conditions anomalies on land energy balance,
373 particularly on the surface fluxes sensible and latent heat. Figure 14 shows changes in sensible
374 heat fluxes (in $W.m^{-2}$) for JJAS 2003 and JJAS 2004, from dry and wet experiments compared to
375 their corresponding control experiments, and the dotted area shows changes that are statistically
376 significant at the 0.05 level. As can be seen in figure 14, the soil moisture initial conditions
377 anomalies strongly affect the sensible fluxes.

378 In the dry experiments, the increase of sensible heat flux changes are located under the latitude
379 $15^{\circ}N$, while the decrease of sensible heat flux changes are found over most of area above the
380 latitude $15^{\circ}N$ for both JJAS 2003 and JJAS 2004 (Fig.14a, c). Conversely, in wet experiments we
381 have a dominant decrease of sensible heat flux changes, found over almost whole West Africa
382 domain except the orographic and somewhat along Guinea coastline for both JJAS 2003 and JJAS
383 2004 (see Fig 14b, d).

384 The PDF distributions of the change in sensible heat flux are displayed in Figure 15. The dry (wet)
385 experiments show an increase (decrease) of the sensible flux in both JJAS 2003 and JJAS 2004
386 over all the domains studied (Fig. 15). The impact in wet experiments is strong compared to the
387 dry experiments over central and west Sahel except over Guinea coast (Fig. 15). Overall, the
388 impact on sensible heat flux of soil moisture initial conditions anomalies is homogeneous, i.e., dry
389 experiments tend to cause an increase of sensible heat flux while the wet experiments tend to favor
390 a decrease of sensible heat flux over most of the domains studied. The strongest impacts on
391 sensible heat flux in wet and dry experiments are found over respectively west Sahel and Guinea
392 coast, with peak modes about respectively $-40W.m^{-2}$ and $10W.m^{-2}$ (resp. Fig. 15,b and Fig. 15c).

393 Unlike the case of sensible heat flux, changes in latent heat show opposite patterns, we found a
394 dominant decrease (increase) of latent heat flux in dry (wet) experiment over almost all of the
395 studied domains. Nevertheless, in the dry experiments, we found a sparse increase of latent heat
396 over the Sahara and Senegal (Fig.16b, d), while in wet experiment a sparse decrease is located
397 over the Guinea coast (Fig.16b, d). The PDF distributions of latent heat flux change are shown in
398 Figure 17. It can be seen that the impact on latent heat flux of soil moisture anomalies is
399 homogeneous, i.e. dry experiments result to a decrease in latent heat flux while the wet
400 experiments result in an increase in the latent heat flux over most of the domains studied. The

401 strongest impact on latent heat flux in wet and dry experiments are found over respectively west
402 Sahel and Guinea coast with peaks mode at $40W.m^{-2}$ and $-15W.m^{-2}$ (resp. Fig. 17 b and Fig. 17 c).
403 Overall, the impacts in wet experiments on latent and sensible heat flux are strong compared to
404 the dry experiments over most of the domains studied, except over Guinea coast (Fig. 17).
405 In order to know whether most of the changes in energy go to evaporating water or to heating the
406 environment, we analyzed in Fig. 18 the changes in Bowen ratio for JJAS 2003 and JJAS 2004,
407 from dry and wet experiments with respect to their corresponding control experiments. The dotted
408 area displays differences that are statistically significant at the 0.05 level. The soil moisture
409 anomalies strongly affected the Bowen ratio. The dry experiments show a dominant increase of
410 evaporation energy (Bowen ratio value in the range $[0,1]$) under the latitude $15^{\circ}N$ for both JJAS
411 2003 and JJAS 2004 (Fig.18a, c). However, above latitude $15^{\circ}N$ we found a mixture of increasing
412 and decreasing energy for environment heating (Bowen ratio value more than ± 1) (Fig.18a, c).
413 For the wet experiments (Fig.18b, d), we found a dominant decrease of energy for environment
414 heating above the latitude $14^{\circ}N$ (Bowen ratio less than -1), while under this latitude, we found a
415 mixture of decrease and increase in evaporation energy (Bowen ratio in the range $[-1; 1]$). As
416 expected, the areas where most of the energy changes go to water evaporation are generally
417 coincident with areas of temperature changes. The decrease (increase) in evaporation area
418 coincides with decrease (increase) of temperature change.
419 For a quantitative evaluation, the PDF distribution of the Bowen ratio is shown in Figure 18. Over
420 the Guinea coast, for both dry and wet experiments, most of the energy go to evaporation with
421 decrease in Bowen ratio about, the dry (wet) experiments show an increase (decrease) of water
422 evaporation energy about 0.12 (-0.1) in both JJAS 2003 and JJAS 2004 (Fig. 19c).
423 On other hand, over the central Sahel (Fig.19 a), for the dry and wet experiments, most of the
424 energy goes to evaporation. The dry (wet) experiments further increase (decrease) the evaporative
425 energy with pic at 0.4 (-0.7) for both JJAS 2003 and JJAS 2004 over the central Sahel. In contrast,
426 in wet (dry) experiments over west Sahel (Fig. 19b), most of the energy goes to heat the
427 environment (to evaporation) with a decrease in Bowen ratio about -3 (-0.1).
428 We now examine the impact on the stability of planetary boundary layer (PBL) of the anomalies
429 in soil moisture initial conditions. Soil moisture can influence rainfall by limiting
430 evapotranspiration, which affects the development of the daytime planetary boundary layer and
431 thereby the initiation and intensity of convective precipitation (Eltahir, 1998). Figure 20 shows the
432 changes in PBL (in m) for JJAS 2003 and JJAS 2004, from dry and wet experiments with respect
433 to their corresponding control experiments with dotted areas that are statistically significant at the
434 0.05 level. The soil moisture anomalies impact significantly the PBL. The dry experiments show

435 an increase of the PBL under the latitude 15°N , except a western part of west Sahel, while a
436 dominant decrease of PBL is shown above this latitude for both JJAS 2003 and JJAS 2004 (resp.
437 Fig.20 a and c). For the wet experiments, a decrease of PBL is located over most of the domains
438 studied, however a sparse increase is found above the latitude 15°N . The PDF distribution of PBL
439 changes, computed over the area indicated in Figure1 is shown in Figure 21. The impact on PBL
440 is homogeneous over most of the domains studied (Fig.21). The dry (wet) experiments lead to an
441 increase (decrease) of PBL for both JJAS 2003 and JJAS 2004 over most of the domains studied.
442 The strongest impacts on PBL, in the wet and dry experiments, are found over respectively the
443 west Sahel and Guinea coast, about respectively -300 m and 150m. There is a dry (wet) air above
444 the area where there is increase (decrease) of PBL, which results in warm (cool) and dry (moist)
445 over most of the domains studied (see Fig. 8 and Fig. 9). These results are consistent with the work
446 of Han and Pan 2003.

447 Summarizing the results of this section, simultaneously the cooling of surface temperature is
448 associated with a decrease in latent heat, and increase in sensible heat and the PBL over most of
449 the domain studied. Conversely the warming of surface temperature is associated with an increase
450 in latent heat and decrease in sensible heat and the PBL height. These results are consistent with
451 previous work of Eltahir et al. (1998). Furthermore, sensible and latent heat fluxes, Bowen ratio
452 and PBL responses to the anomalies in soil moisture initial conditions are somewhat sensitive to
453 the contrast of year and experiments (wet and dry).

454

455 **4. Conclusion**

456 The impact of the anomalies in soil moisture initial conditions on the subsequent summer mean
457 climate over West Africa is explored using the RegCM4-CLM45. Particularly, the aim of this
458 study was to investigate how soil moisture initialization at the beginning of the rainy season may
459 impact the intraseasonal variability of temperature and precipitation mean within the subsequent
460 season (June to September). For this purpose, three (3) experiments each with simulations starting
461 from June 1st to September 30th were set up and runs were performed in JJAS 2003 and in JJAS
462 2004. The difference between these 3 experiments is on the change of soil moisture initial
463 condition at the beginning of the simulation: For each experiment, we applied (i) a control soil
464 moisture initial condition, (ii) then a wet soil moisture initial condition, and (iii) a dry soil moisture
465 initial condition.

466 The impact of soil moisture initial condition on precipitation depends on the location, the
467 magnitude and on the persistence of the anomalies of soil moisture initial condition throughout the

468 season. Over the West Sahel and the Guinea coast, both dry and wet experiments lead to an
469 increase of precipitation stronger in the wet experiment with a peak of change of 40% noted in the
470 West Sahel. Over the Central Sahel, the wet experiment lead to an increase of precipitation with a
471 peak of change around 15% while the dry experiments lead to a decrease of precipitation with a
472 peak of change not exceeding 10%. Anomalies of soil moisture initial condition can persist for
473 three to four months (90-120 days) depending the region of West Africa but the impact on
474 precipitation is no longer than 30 days (15 days over the Sahel and 30 days over the Guinea Sahel).
475 Our results indicate that a wet soil moisture initial condition lead in the low levels of the
476 atmosphere to an increase of relative humidity associated with a cooling of temperature and in the
477 upper levels, to a decrease of relative humidity and a warming, while the dry experiment mainly
478 impact the lower levels with a decrease of the relative humidity associated with a warming.
479 However, over the West Sahel and Guinea coast, the increase of precipitation shown in the dry
480 experiments may result from the transport of moisture from the Atlantic Ocean by westerlies. The
481 temperature is more sensitive to the anomalies of soil moisture initial condition than precipitation.
482 The strongest impacts are located over the Central Sahel with the peak of change of $-1.5\text{ }^{\circ}\text{C}$ and
483 0.5°C respectively in wet and dry experiments. Moreover, the soil moisture initial conditions
484 influence the surface fluxes such as the sensible and latent heat, the Bowen ratio and the PBL
485 height.

486 The main conclusion of our study shows that soil moisture as a boundary condition plays a major
487 role in controlling summer climate variability not only over the transition zone of climate but also
488 over humid zone such as Guinea Coast. This study demonstrates that a good prescription of the
489 initial condition of soil moisture can improve the simulation of the precipitation and air
490 temperature, then would help to reduce biases in climate model simulations. Overall, land surface
491 initialization can contribute to improve subseasonal to seasonal forecast skill, but this needs to be
492 investigated further. We recognize that sensitivity experiments such as "wet" and "dry" ones
493 conducted in this study were not intended to simulate real climate since such extremes are very
494 rare. These kinds of experiments, however, can provide estimates of the limits of the impact of
495 internal forcing of the soil moisture on the new non-hydrostatic dynamical core of RegCM4.
496 Finally, in a context of climate change with projected increase of high impact weather events in
497 the region, there is a need to explore the sensitivity of soil moisture initial conditions on climate
498 extremes.

499

500 **Authors contributions**

501 The authors declare to have no conflict of interest with this work. B. Koné and A. Diedhiou fixed
502 the analysis framework. B. Koné carried out all the simulations and figures production
503 according to the outline proposed by A. Diedhiou. B. Koné and A. Diedhiou, S. Anquetin and A.
504 Diawara worked on the analyses. All authors contributed to the drafting of this manuscript.

505 **Acknowledgements**

506 The research leading to this publication is co-funded by the NERC/DFID “Future Climate for
507 Africa” programme under the AMMA-2050 project, grant number NE/M019969/1 and by IRD
508 (Institut de Recherche pour le Développement; France) grant number UMR IGE Imputation
509 252RA5.

510 **References:**

511
512 Beljaars A. C. M., Viterbo P. , Miller M. J., and Betts A. K.: The anomalous rainfall over the
513 United States during July 1993: Sensitivity to land surface parameterization and soil moisture
514 anomalies, *Mon. Weather Rev.*, 124(3), 362–382, doi:10.1175/1520-0493(1996)124<0362:
515 TAROTU>2.0.CO;2, 1996.

516
517 Bosilovich, M. G., and Sun W. Y.: Numerical simulations of the 1993 Midwestern flood: Land–
518 atmosphere interactions. *J. Climate*, 12, 1490–1505, 1999.

519
520 Cook K. H.: Generation of the African easterly jet and its role in determining West African
521 precipitation, *J. Climate*, 12, 1165–1184, [https://doi.org/10.1175/1520-0442](https://doi.org/10.1175/1520-0442(1999)012) (1999)012
522 <1165:GOTAEJ> 2.0.CO;2, 1999.

523
524 Danielson J.J., and Gesch D.B.: Global multi-resolution terrain elevation data 2010
525 (GMTED2010): U.S. Geological Survey Open-File Report 2011–1073, 26 p, 2011.

526
527 Dirmeyer P. A., Koster R. D., and Guo Z.: Do global models properly represent the feedback
528 between land and atmosphere?, *J. Hydrometeorol.*, 7(6), 1177–1198, doi:10.1175/JHM532.1,
529 2006.

530
531 Douville, F. Chauvin, and H. Broqua.: Influence of soil moisture on the Asian and African
532 monsoons. Part I: Mean monsoon and daily precipitation. *J. Climate*, 14, 2381–2403, 2001.

533

534 Eltahir E. A. B.: A soil moisture-rainfall feedback mechanism 1. Theory and observations, *Water*
535 *Resour. Res.*, 34, 765–776, doi:10.1029/97WR03499, 1998.

536

537 Emanuel K. A.: A scheme for representing cumulus convection in large-scale models. *Journal of*
538 *the Atmospheric Science* 48: 2313–2335, 1991.

539

540 Fan Y., and van den Dool H.: A global monthly land surface air temperature analysis for 1948 -
541 present, *J. Geophys. Res.* 113, D01103, doi: 10.1029/2007JD008470, 2008.

542

543 Gao, X.-J., Shi, Y., and Giorgi, F.: Comparison of convective parameterizations in RegCM4
544 experiments over China with CLM as the land surface model, *Atmos. Ocean. Sci. Lett.*, 9, 246–
545 254, <https://doi.org/10.1080/16742834.2016.1172938>, 2016.

546

547 Giorgi F., Coppola E., Solmon F., Mariotti L., Sylla M. B., Bi X., Elguindi N., Diro G. T., Nair
548 V., Giuliani G., Cozzini S., Guettler I., O’Brien T., Tawfik A., Shalaby A., Zakey A. S., Steiner
549 A., Stordal F., Sloan L., and Brankovic C.: RegCM4: model description and preliminary tests
550 over multiple CORDEX domains, *Clim. Res.*, 52, 7–29, <https://doi.org/10.3354/cr01018>, 2012.

551

552 Grell G., Dudhia J. and Stauffer D. R.: A description of the fifth generation Penn State/NCAR
553 Mesoscale Model (MM5), National Center for Atmospheric Research Tech Note NCAR/TN-
554 398+STR, NCAR, Boulder, CO, 1994.

555

556 Harris I., Jones P. D., Osborn T. J. and Lister D. H.: Updated high-resolution grids of monthly
557 climatic observations, *Int. J. Climatol.*, 34, 623–642, <https://doi.org/10.1002/joc.3711>, 2013.

558

559 Holtslag A., De Bruijn E., and Pan H. L.: A high resolution air mass transformation model for
560 short-range weather forecasting, *Mon. Weather Rev.*, 118, 1561–1575, 1990.

561

562 Hong S-Y. and Pan H-L.: Impact of soil moisture anomalies on seasonal, summertime circulation
563 over North America in a regional climate model. *J. Geophys. Res.*, 105 (D24), 29 625–29 634,
564 2000.

565

566 Huffman G. J., Adler R. F., Bolvin D. T., Gu G., Nelkin E. J., Bowman K. P., Hong Y, Stocker E.
567 F., and Wolff D. B.: The TRMM multisatellite precipitation analysis: quasi-global, multi-year,
568 combined-sensor precipitation estimates at fine scale, *J. Hydrometeorol.*, 8, 38-55, 2007.

569

570 Jaeger E. B., and Seneviratne S.I.: Impact of soil moisture-atmosphere coupling on European
571 climate extremes and trends in a regional climate model, *Clim. Dyn.*, 36(9-10), 1919-1939,
572 doi:10.1007/s00382-010-0780-8, 2011.

573

574 Kang S, Im E.-S. and Ahn J.-B.: The impact of two land-surface schemes on the characteristics
575 of summer precipitation over East Asia from the RegCM4 simulations *Int. J. Climatol.* 34: 3986-
576 3997, 2014.

577

578 Kiehl J., Hack J., Bonan G., Boville B., Breigleb B., Williamson D., Rasch P. ; Description of the
579 NCAR Community Climate Model (CCM3). National Center for Atmospheric Research Tech
580 Note NCAR/TN-420+STR, NCAR, Boulder, CO, 1996.

581

582 Kim J-E., and Hong S-Y.: Impact of Soil Moisture Anomalies on Summer Rainfall over East Asia:
583 A Regional Climate Model Study, *Journal of Climate.* Vol. 20, 5732–5743, DOI:
584 10.1175/2006JCLI1358.1, 2006.

585

586 Kirtman B.P., Schopf P. S.: Decadal Variability in ENSO Predictability and Prediction. *Journal*
587 *of Clim.* 11, 2804, 1998.

588

589 Koné B., Diedhiou A., N’datchoh E. T., Sylla M. B., Giorgi F., Anquetin S., Bamba A., Diawara
590 A., and Koba A. T.: Sensitivity study of the regional climate model RegCM4 to different
591 convective schemes over West Africa. *Earth Syst. Dynam.*, 9, 1261–1278.
592 <https://doi.org/10.5194/esd-9-1261-2018>, 2018.

593

594 Koster R. D., Dirmeyer P. A., Zhichang G., Bonan G., Chan E., Cox P., Gordon C. T., Kanae S.,
595 Kowalczyk E., Lawrence D., Liu P., Lu C. H, Malyshev S., McAvaney B., Mitchell K, Mocko D.,
596 Oki T., Oleson K., Pitman A., Sud Y. C. , Taylor C. M., Versegny D., Vasic R., Xue Y., Yamada
597 T.: Regions of strong coupling between soil moisture and precipitation, *Science*, 305, 1138–1140,
598 doi:10.1126/science.1100217, 2004.

599

600 Lawrence D.M., Oleson K.W., Flanner M.G., Thornton P.E., Swenson S.C., Lawrence P.J. , Zeng
601 X., Yang Z.-L., Levis S., Sakaguchi K., Bonan G.B., and Slater A.G.:Parameterization
602 improvements and functional and structuraladvances in version 4 of the Community Land Model.
603 J. Adv. Model. Earth Sys. 3. DOI:10.1029/2011MS000045, 2011.

604

605 Liu D., WangG. L., Mei R. , Yu Z. B. and Gu H. H.: Diagnosing the strength of land-atmosphere
606 coupling at sub-seasonal to seasonal time scales in Asia, J. Hydrometeor., doi:10.1175/JHM-D-
607 13-0104.1, 2013.

608

609 Liu D., G. Wang R. Mei Z. Yu, and Yu M.: Impact of soil moisture initial conditions anomalies
610 on climate mean and extremes over Asia, J. Geophys. Res. Atmos., 119, 529–545,
611 doi:10.1002/2013JD020890, 2014.

612

613 Loveland, T. R., Reed, B. C., Brown, J. F., Ohlen, D. O., Zhu, J., Yang, L., and Merchant, J. W.:
614 Development of a global land cover characteristics database and IGBP DISCover from 1-km
615 AVHRR Data, Int. J. Remote. Sens., 21, 1303–1330, 2000.

616

617 Oglesby R. J., and Erickson III D. J.: Soil moisture and the persistence of North American drought.
618 J. Climate, 2, 1362–1380, 1989.

619

620 Oglesby R. J., Marshall S. , Erickson III D. J., Roads J. O. and Robertson F. R.: Thresholds in
621 atmosphere-soil moisture interactions: Results from climate model studies. J. Geophys. Res.,107,
622 4244, doi:10.1029/2001JD001045, 2002.

623

624 Oleson K., Lawrence D. M., Bonan G. B., Drewniak B., Huang M., Koven C. D., Yang Z. -L.:
625 Technical description of version 4.5 of the Community Land Model (CLM) (No. NCAR/TN-
626 503+STR). doi:10.5065/D6RR1W7M, 2013.

627

628 Paeth H., Girmes R., Menz G. and Hense A.: Improving seasonal forecasting in the low latitudes,
629 Mon. Weather Rev., 134, 1859-1879, 2006.

630

631 Pal J. S., Small E. E. and Elthair E. A.: Simulation of regional scale water and energy budgets:
632 representation of subgrid cloud and precipitation processes within RegCM, J. Geophys. Res., 105,
633 29579–29594, 2000.

634
635 Pal J. S. and Eltahir E. A. B.: Pathways relating soil moisture conditions to future summer rainfall
636 within a model of the land–atmosphere system. *J. Climate*, 14, 1227–1242, 2001.
637
638 Peterson T. C., Folland C., Gruza G., Hogg W. Mokssit A., Plummer N.: Report on the activities
639 of the working group on climate change detection and related rapporteurs 1998-2001. Geneva
640 (Switzerland): WMO Rep. WCDMP 47, WMO-TD 1071, 2001.
641
642 Nicholson S. E.: The West African Sahel: a review of recent studies on the rainfall regime and its
643 interannual variability, *Meteorology*, 453521, 32 p., <https://doi.org/10.1155/2013/453521>, 2013.
644 Nikulin G., Jones C., Samuelsson P., Giorgi F., Asrar G., Büchner M., Cerezo-Mota R.,
645 Christensen O. B., Déque M., Fernandez J., Hansler A., van Meijgaard E., Sylla M. B. and
646 Sushama L.: Precipitation climatology in an ensemble of CORDEX-Africa regional climate
647 simulations, *J. Climate*, 6057–6078, <https://doi.org/10.1175/JCLI-D-11-00375.1>, 2012.
648
649 Rasmusson E. M. and Carpenter T. H.: Variations in Tropical Sea Surface Temperature and
650 Surface Wind Fields Associated with the Southern Oscillation/El Niño. *Mon. Weather Rev.* 110,
651 354, 1982.
652
653 Reynolds, R. W. and Smith, T. M.: Improved global sea surface temperature analysis using
654 optimum interpolation, *J. Climate*, 7, 929–948, 1994.
655
656 Seager R., and Vecchi G. A.: Greenhouse warming and the 21st century hydroclimate of
657 southwestern North America. *Proc. Natl. Acad. Sci. USA*, 107, 21 277–21 282,
658 doi:10.1073/pnas.0910856107, 2010.
659
660 Simmons A. S., Uppala D. D. and Kobayashi S.: ERA-interim: new ECMWF reanalysis products
661 from 1989 onwards, *ECMWF Newsl.*, 110, 29–35, 2007.
662
663 Solmon F., Giorgi F., and Lioussse C.: Aerosol modeling for regional climate studies: application
664 to anthropogenic particles and evaluation over a European/African domain, *Tellus B*, 58, 51–72,
665 2006.

666
667 Sundqvist H. E., Berge E., and Kristjansson J. E.: The effects of domain choice on summer
668 precipitation simulation and sensitivity in a regional climate model, *J. Climate*, 11, 2698-2712,
669 1989.

670
671 Thorncroft, C. D. and Blackburn, M.: Maintenance of the African easterly jet, *Q. J. R. Meteorol*
672 *Soc.*, 125, 763–786, 1999.

673
674 Uppala S., Dee D., Kobayashi S., Berrisford P. and Simmons A.: Towards a climate data
675 assimilation system: status update of ERA-interim, *ECMWF Newsl.*, 15, 12–18, 2008.

676
677 Vinnikov K. Y. and Yeserkepova I. B.: Soil moisture: Empirical data and model results, *J. Clim.*,
678 4(1), 66–79, doi:10.1175/1520-0442(1991)004<0066:SMEDAM>2.0.CO;2, 1991.

679
680 Vinnikov K. Y., Robock A., Speranskaya N. A. and Schlosser A.: Scales of temporal and spatial
681 variability of midlatitude soil moisture, *J. Geophys. Res.*, 101(D3), 7163–7174,
682 doi:10.1029/95JD02753, 1996.

683
684 Wang, G., Yu, M., Pal, J. S., Mei, R., Bonan, G. B., Levis, S., and Thornton, P. E.: On the
685 development of a coupled regional climate vegetation model RCM-CLM-CN-DV and its
686 validation its tropical Africa, *Clim. Dynam*, 46, 515–539, 2016.

687
688 Xue Y., De Sales F., Lau K. M. W., Bonne A., Feng J., Dirmeyer P., Guo Z., Kim K. M., Kitoh
689 A., Kumar V., Pocard-Leclercq I., Mahowald N., Moufouma-Okia W., Pegion P., Rowell D. P.,
690 Schemm J., Schulbert S., Sealy A., Thiaw W. M., Vintzileos A., Williams S. F. and Wu M. L.:
691 Intercomparison of West African Monsoon and its variability in the West African Monsoon
692 Modelling Evaluation Project (WAMME) first model Intercomparison experiment, *Clim. Dynam.*,
693 35, 3–27, <https://doi.org/10.1007/s00382-010-0778-2>, 2010.

694
695 Zakey A. S., Solmon F., and Giorgi F.: Implementation and testing of a desert dust module in a
696 regional climate model, *Atmos. Chem. Phys.*, 6, 4687–4704, [https://doi.org/10.5194/acp-6-4687-](https://doi.org/10.5194/acp-6-4687-2006)
697 2006, 2006.

698

699 Zeng X., Zhao M. and Dickinson R .E.: Intercomparison of bulk aerodynamic algorithms for the
 700 computation of sea surface fluxes using TOGA COARE and TAO DATA, J. Climate, 11, 2628-
 701 2644, 1998.

702 Zhang, J., W.-C. Wang, and J. Wei, Assessing land-atmosphere coupling using soil moisture
 703 from the Global Land Data Assimilation System and observational precipitation, J. Geophys.
 704 Res., 113, D17119, doi:10.1029/2008JD009807, 2008.

705 Zhang, J., W.-C. Wang, and L. R. Leung.: Contribution of land-atmosphere coupling to summer
 706 climate variability over the contiguous United States, J. Geophys. Res., 113, D22109,
 707 doi:10.1029/2008JD010136, 2008.

708

709 Zhang, J. Y., L. Y. Wu, and W. Dong,: Land-atmosphere coupling and summer climate variability
 710 over East Asia, J. Geophys. Res., 116, D05117, doi 10.1029/2010JD014714, 2011.

711

712

713

714

715

716

717

718

719

720

721

722

723

724 **Tables and figures:**

725

	Central Sahel		West Sahel		Guinea		West Africa	
	PCC	MB (%)	PCC	MB (%)	PCC	MB (%)	PCC	MB (%)
TRMM 2003	0.98	7.60	0.96	-9.45	0.98	-15.45	0.97	-0.57

CTRL_2003	0.98	-47.97	0.87	-75.76	0.82	-47.12	0.73	-49.31
TMM 2004	0.98	-0.62	0.99	-7.03	0.98	-16.96	0.97	-1.56
CTRL_2004	0.98	-47.89	0.87	-68.35	0.85	-51.97	0.77	-50.56

726

727 **Table1:** The pattern correlation coefficient (PCC) and the mean bias (MB) for JJAS precipitation
728 for model simulation and observation TRMM with respect to CHIRPS, calculated for Guinea
729 coast, central Sahel, west Sahel and the entire West African domain during the period 2003 and
730 2004.

731

732

733

734

735

736

737

738

739

740

741

742

743

Central Sahel		West Sahel		Guinea		West Africa	
PCC	MB (°C)	PCC	MB (°C)	PCC	MB (°C)	PCC	MB (°C)

GTS 2003	0.99	0.31	0.99	0.54	0.99	0.28	0.99	0.39
CTRL_2003	0.99	1.52	0.99	2.68	0.99	-0.34	0.99	0.85
GTS 2004	0.99	0.32	0.99	0.67	0.99	0.28	0.99	0.40
CTRL_2004	0.99	1.50	0.99	2.14	0.99	-0.57	0.99	0.51

744

745 **Table2:** The pattern correlation coefficient (PCC) and the mean bias (MB) for JJAS 2m-
746 temperature for model simulation and observation (GTS) with respect to CRU, calculated for
747 Guinea coast, central Sahel, west Sahel and the entire West African domain during the period 2003
748 and 2004.

749

750

751

752

753

754

755

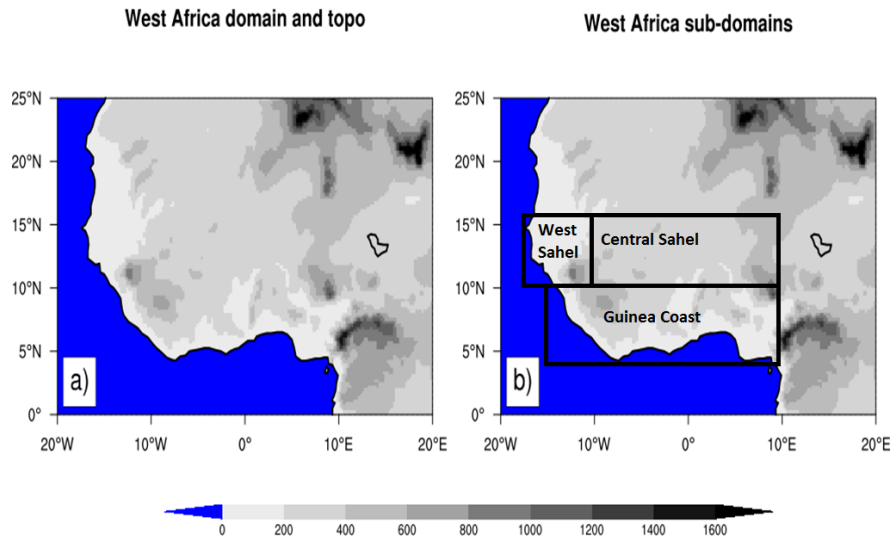
756

757

758

759

760

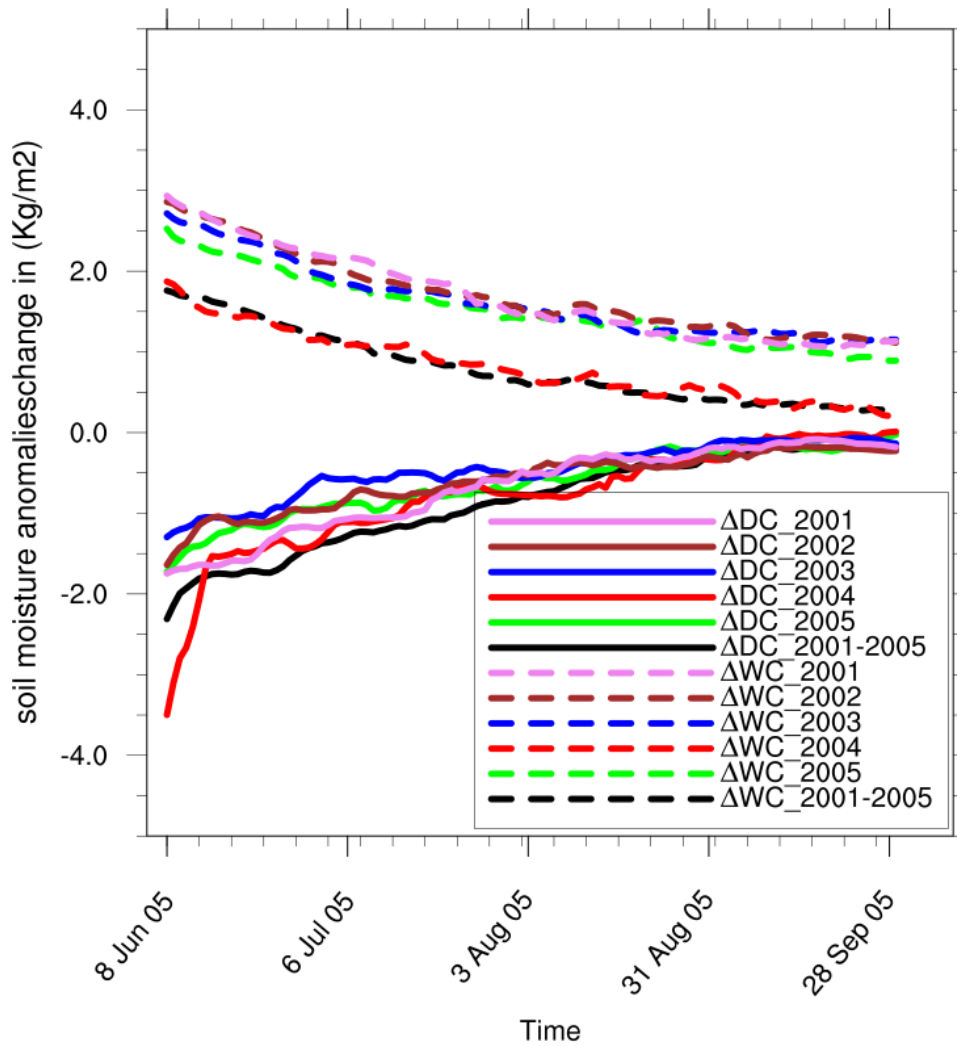


761
762

763 **Figure 1:** Topography of the West African domain. The analysis of the model result has an
764 emphasis on the whole West African domain and the three subregions Guinea coast, central Sahel
765 and west Sahel, which are marked with black boxes.

766
767
768
769
770
771
772
773
774
775
776
777
778
779
780
781
782
783
784
785

West Africa



787
 788 **Figure 2:** Changes in daily soil moisture for 5 years (2001 to 2005) and their climatological mean
 789 during JJAS over West African domain, from dry (ΔDC) and wet (ΔWC) experiments with respect
 790 to their corresponding control experiment.

791

792

793

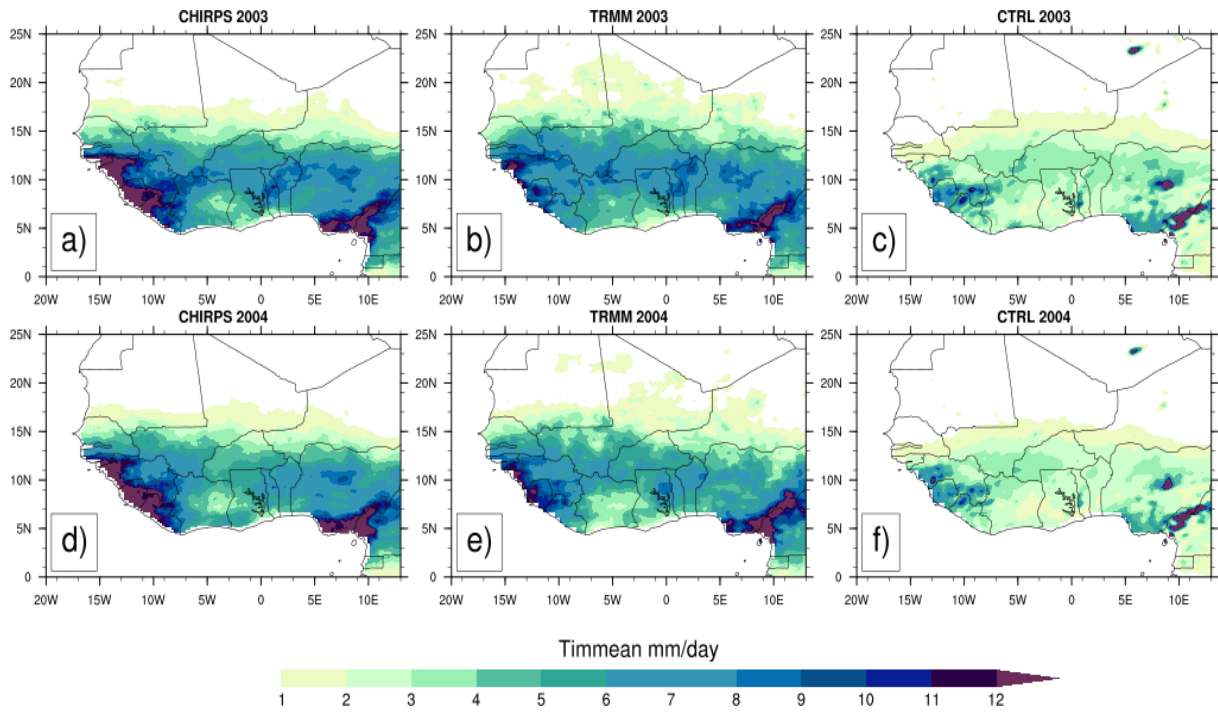
794

795

796

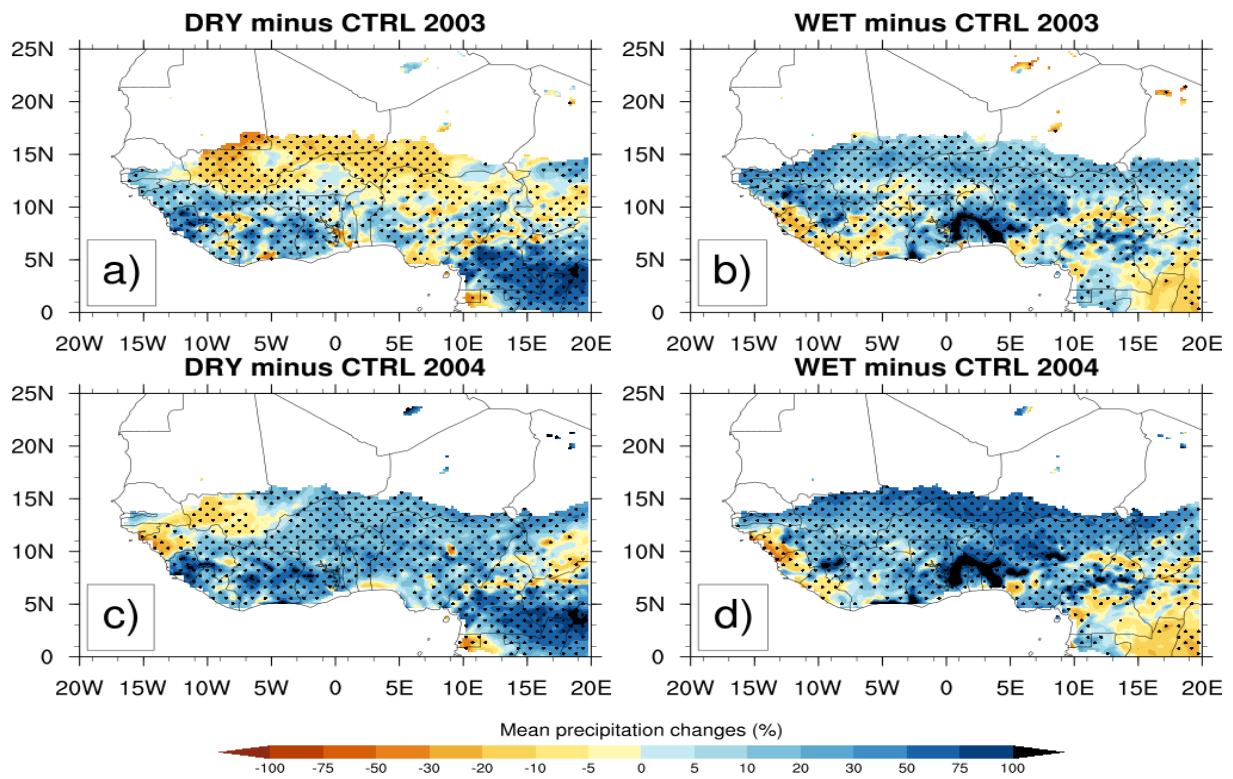
797

798



799
800
801
802
803
804
805
806
807
808
809
810
811
812
813
814
815
816
817

Figure3: Observed 4-month averaged (JJAS) precipitation (mm/day) from CHIRPS (a and d) and TRMM (b and e) for 2003 and 2004 and their corresponding simulated control experiments (CTRL) (c and f) with the reanalysis initial soil moisture ERA20C.



818

819

820 **Figure4:** Changes in mean precipitation (in %) for JJAS 2003 and JJAS 2004, from dry (resp. a
 821 and c) and wet (resp. b and d) experiments with respect to their corresponding control experiment,
 822 the dotted area shows differences that are statistically significant at 0.05 level.

823

824

825

826

827

828

829

830

831

832

833

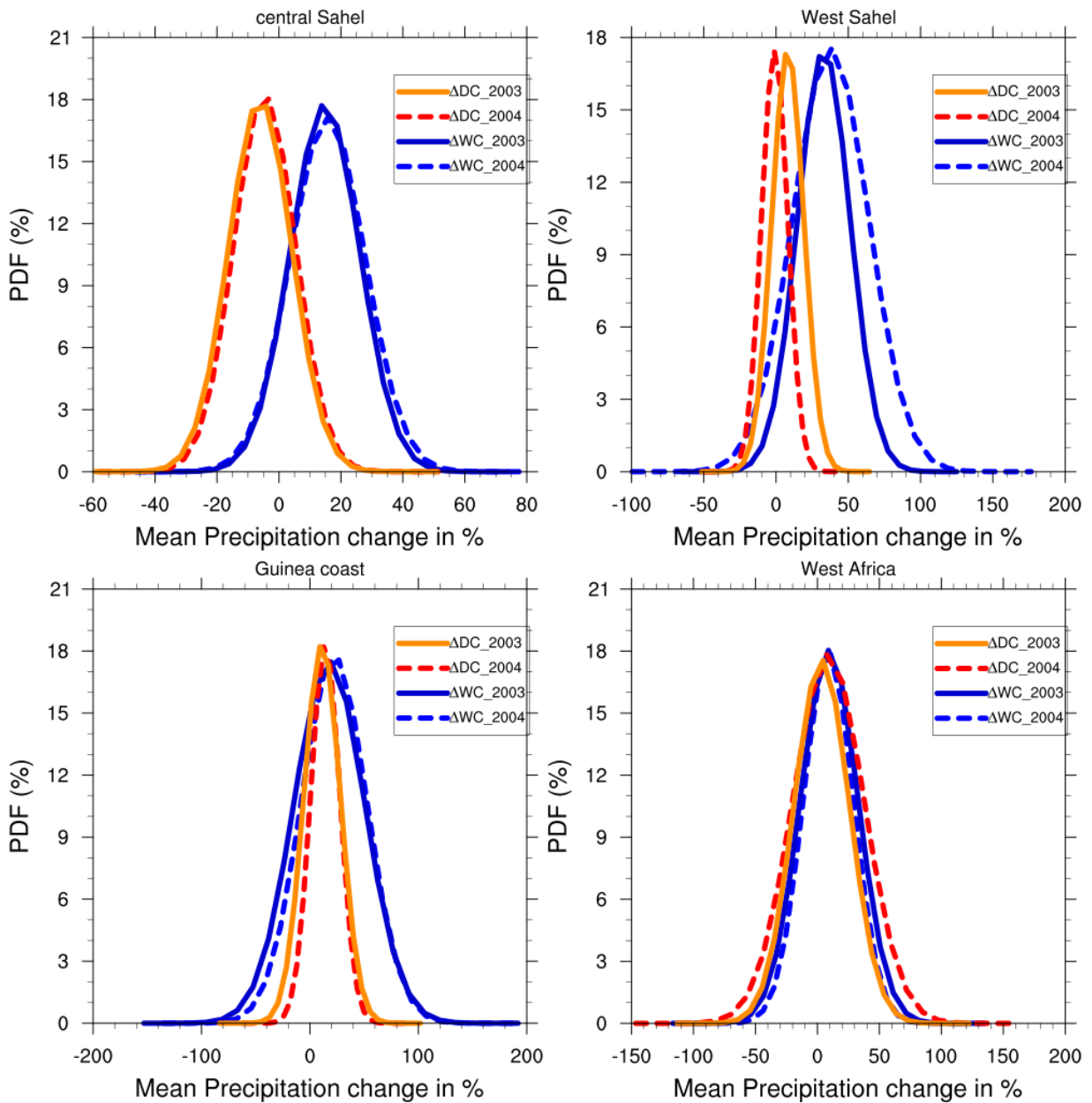
834

835

836

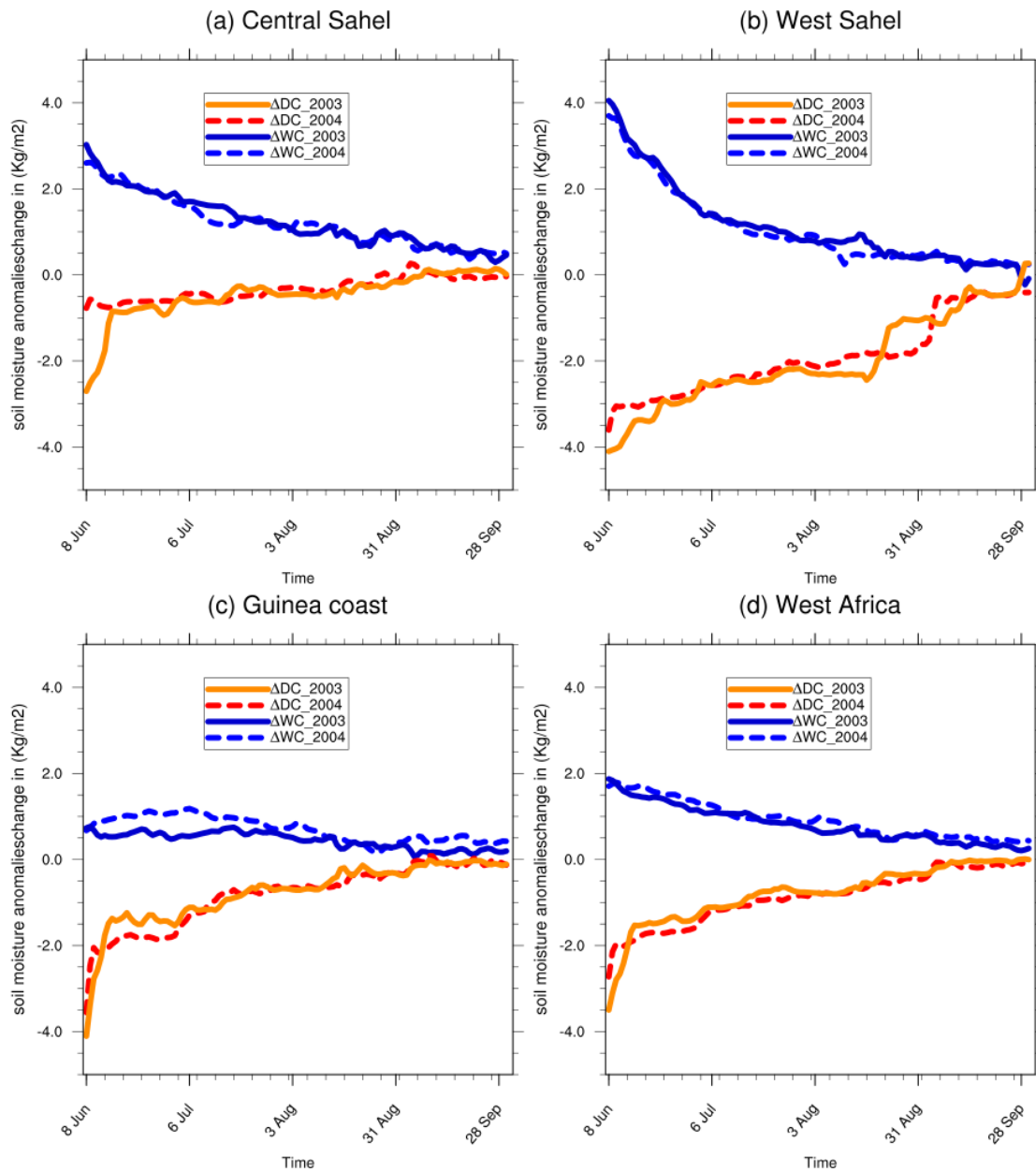
837

838



840
 841 **Figure 5:** PDF distributions (%) of mean precipitation changes in JJAS 2003 and JJAS 2004, over
 842 (a) central Sahel, (b) West Sahel, (c) Guinea and (d) West Africa derived from dry (ΔDC) and wet
 843 (ΔWC) experiments compared to their corresponding control experiment.

844
 845
 846
 847
 848
 849
 850



852

853 **Figure 6:** Daily domain-average soil moisture changes for JJAS 2003 and JJAS 2004, from dry
 854 (ΔDC) and wet (ΔWC) experiments with respect to their corresponding control experiment.

855

856

857

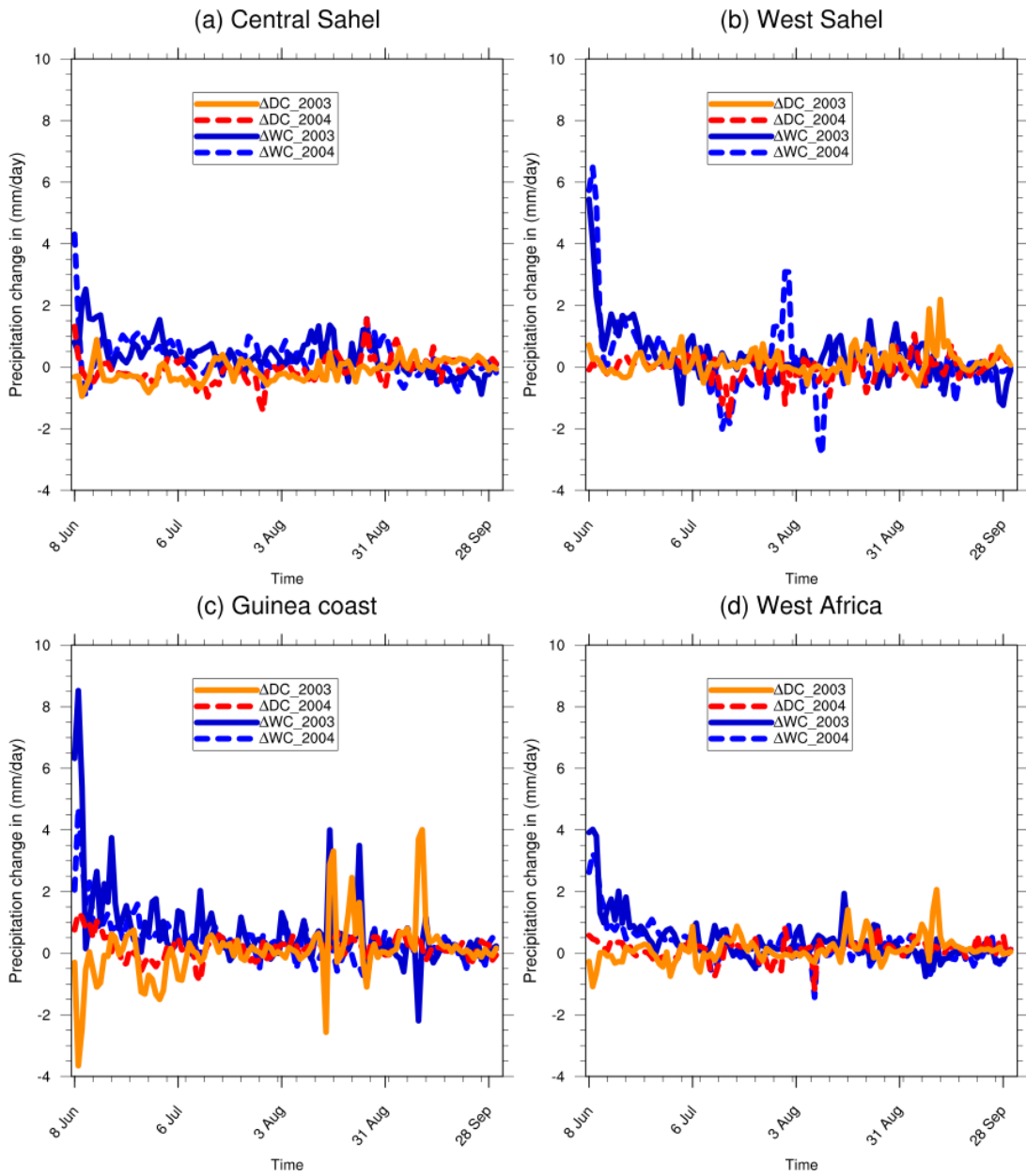
858

859

860

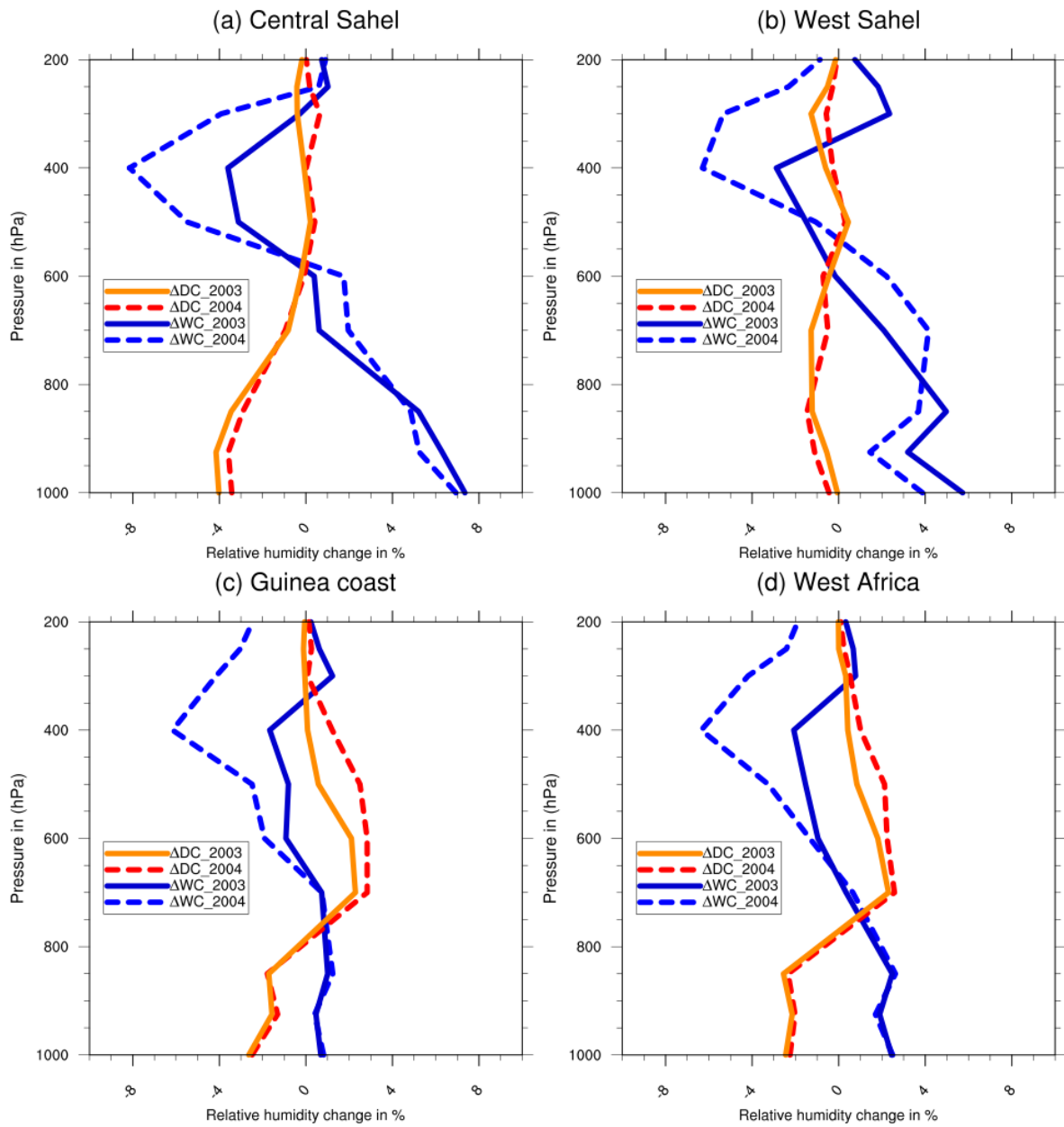
861

862



863
 864
 865
 866
 867
 868
 869
 870
 871
 872
 873
 874

Figure 7: Daily domain-average precipitation changes for JJAS 2003 and JJAS 2004, from dry (ΔDC) and wet (ΔWC) experiments with respect to their corresponding control experiment.



876

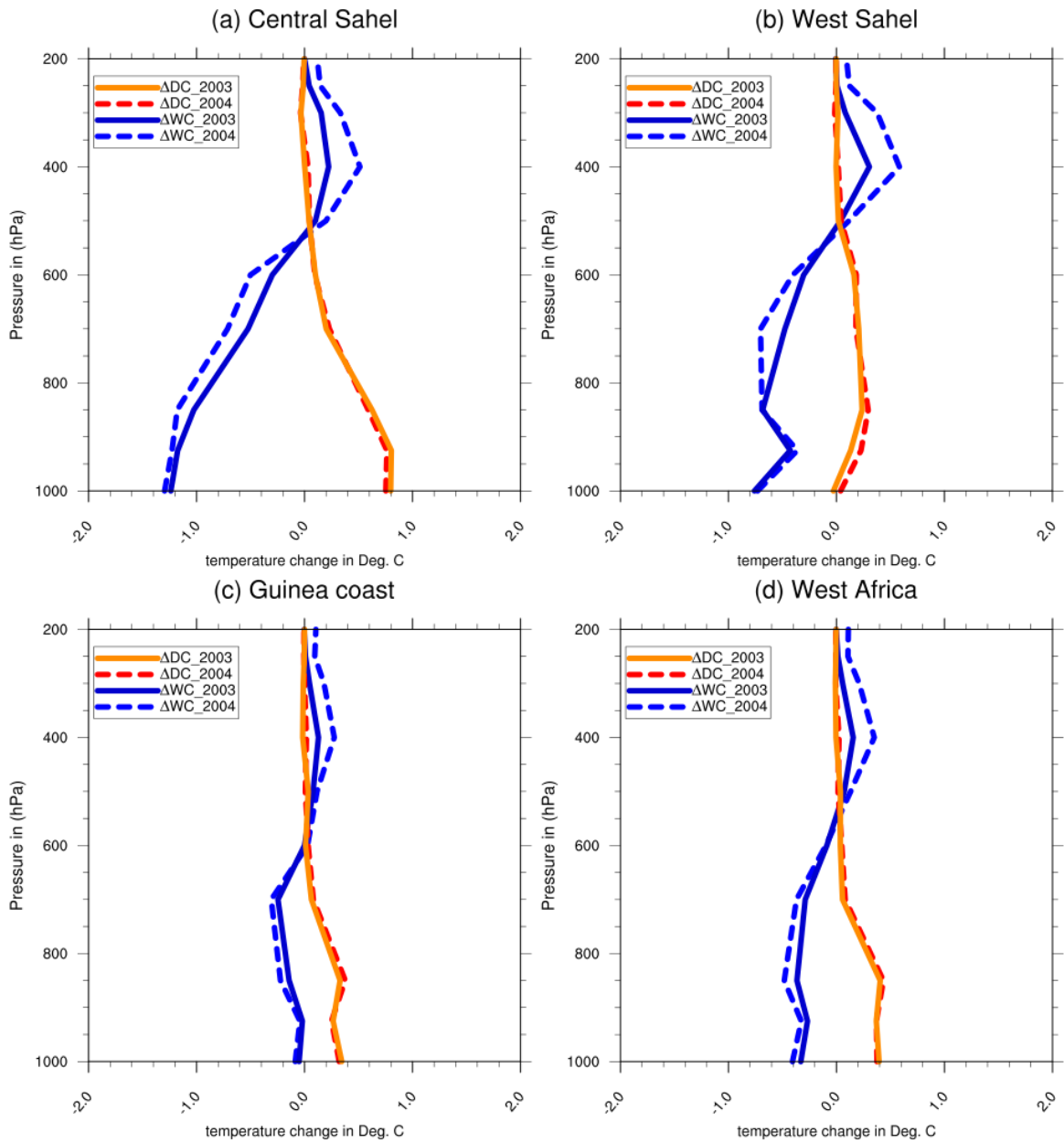
877

878

879 **Figure 8:** Vertical profile changes in Relative humidity for JJAS 2003 and JJAS 2004 from the
 880 dry (ΔDC) and wet (ΔWC) experiments with respect to corresponding control experiment over (a)
 881 central Sahel, (b) west Sahel, (c) Guinea coast, and (d) West Africa.

882

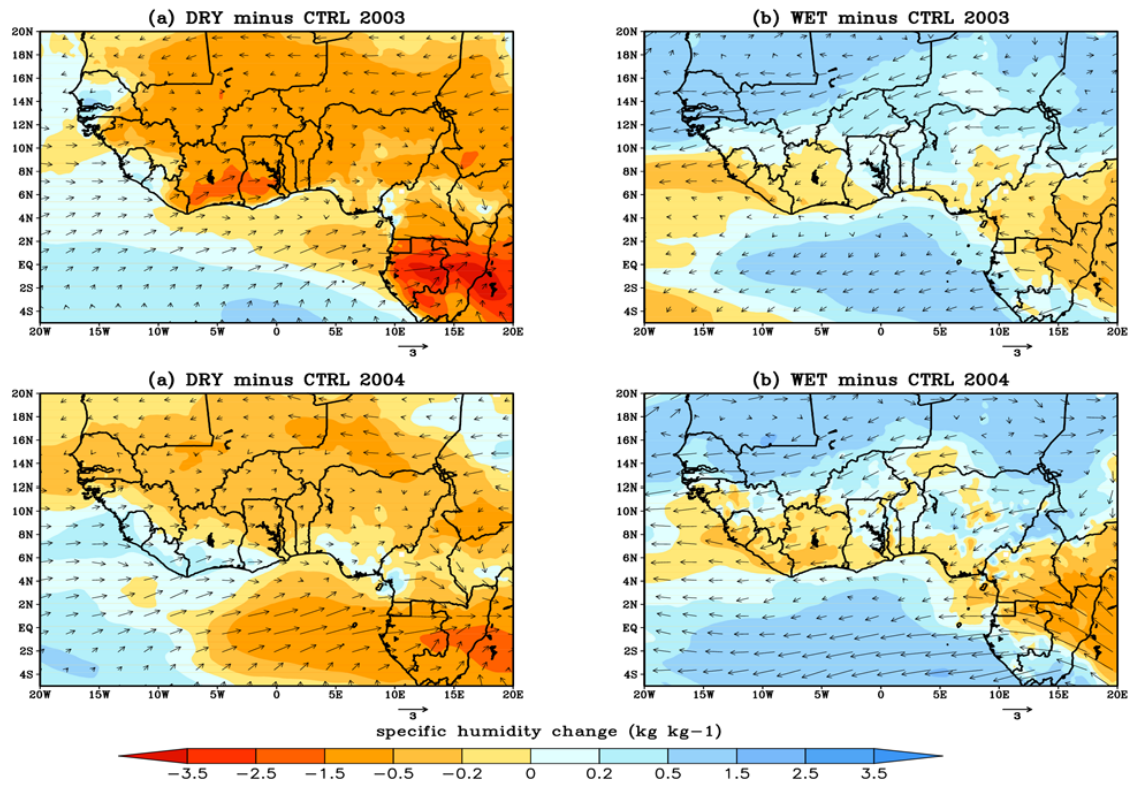
883



884
 885 **Figure 9:** Vertical profile changes in temperature for JJAS 2003 and JJAS 2004 from the dry
 886 (ΔDC) and wet (ΔWC) experiments with respect to their corresponding control experiment over
 887 (a) central Sahel, (b) west Sahel, (c) Guinea coast, and (d) West Africa.

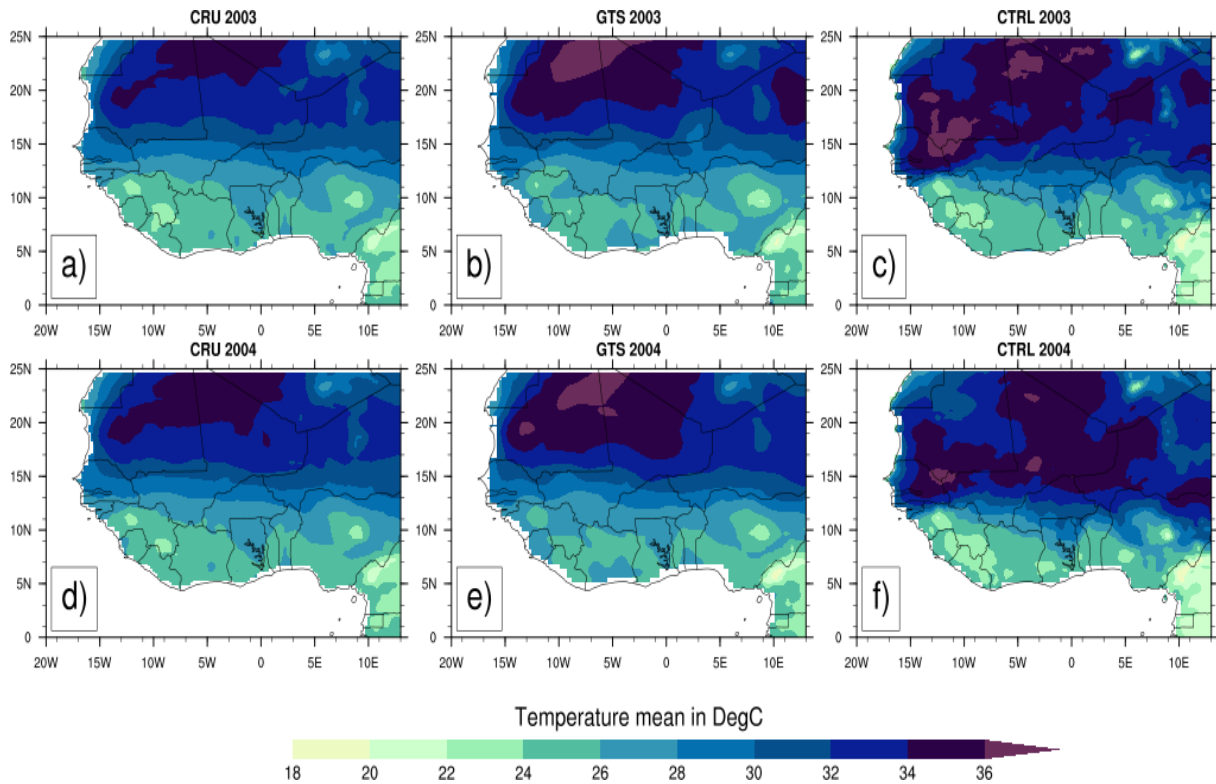
888

889



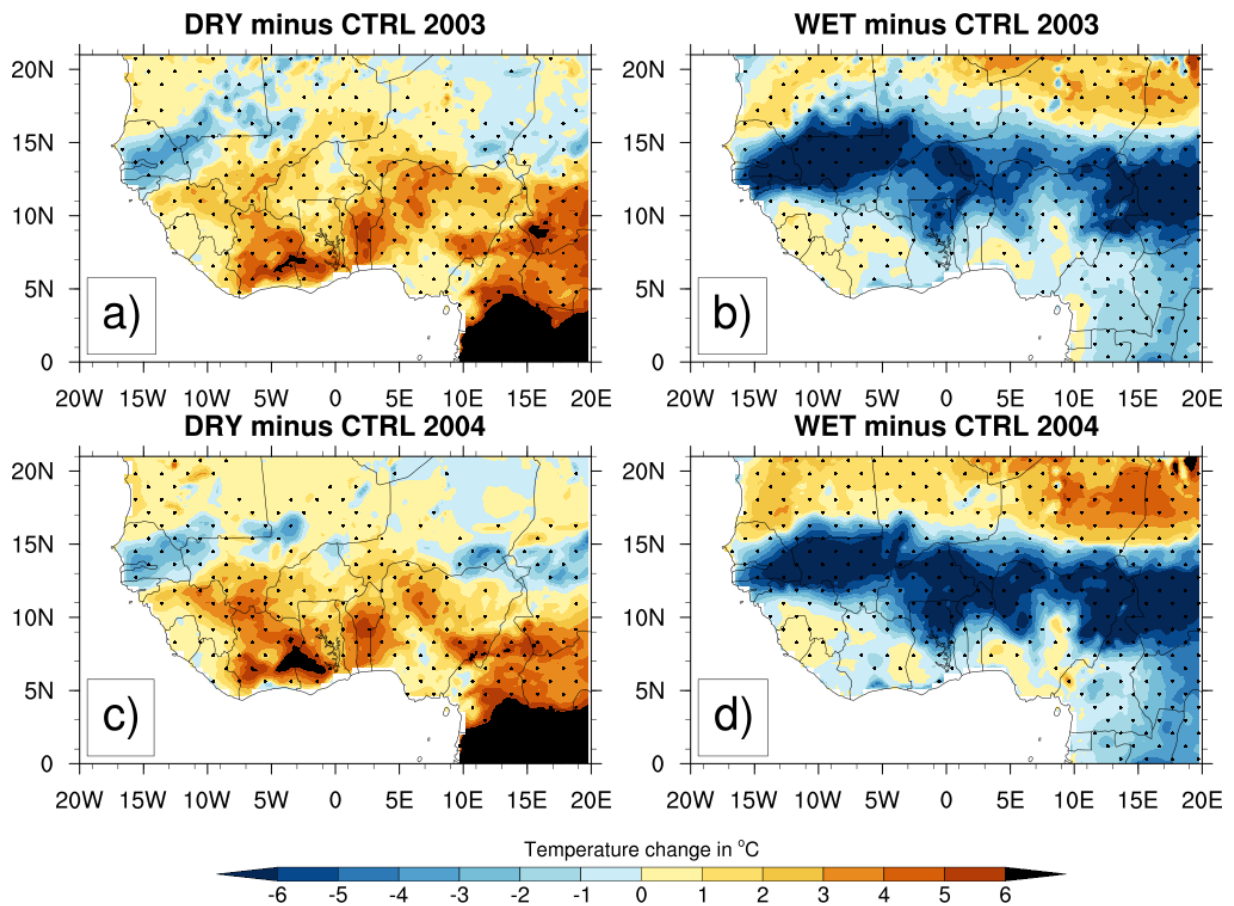
890
 891 **Figure 10:** The lower tropospheric wind (850hpa) and moisture bias for JJAS 2003 and JJAS
 892 2004 from the dry (a and c) and wet (b and d) experiments with respect to their corresponding
 893 control experiment.

894
 895
 896
 897
 898
 899
 900
 901
 902
 903
 904
 905
 906
 907
 908
 909



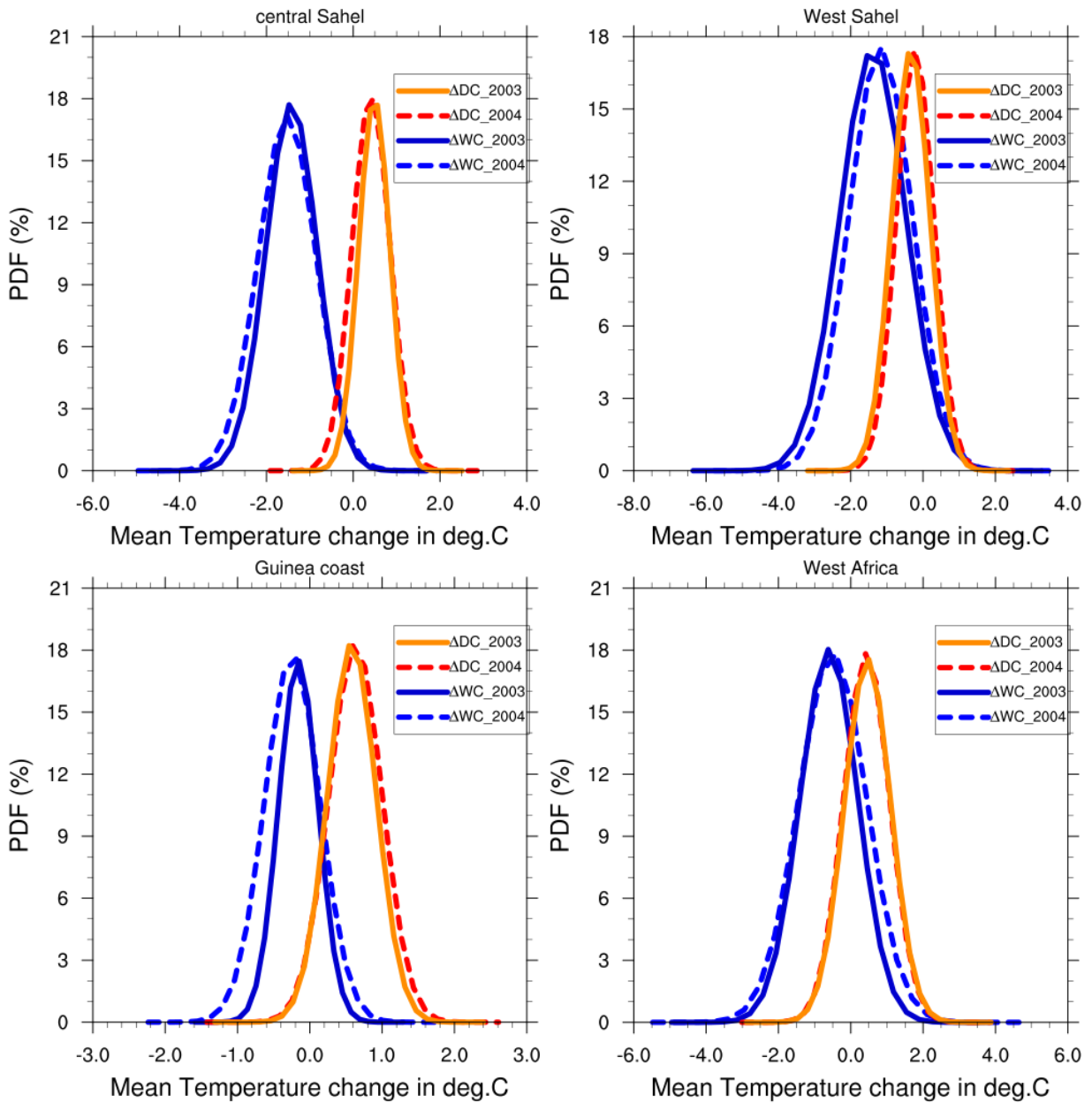
910
 911
 912
 913
 914
 915
 916
 917
 918
 919
 920
 921
 922
 923
 924
 925
 926
 927
 928
 929
 930

Figure 11: Observed 4-month averaged (JJAS) 2m-temperature ($^{\circ}\text{C}$) from CRU (a and d) and GTS (b and e) for 2003 and 2004 and their corresponding simulated control experiment (c and f) with the reanalysis initial soil moisture ERA20C.



931
 932
 933
 934
 935
 936
 937
 938
 939
 940
 941
 942
 943
 944
 945
 946
 947
 948
 949

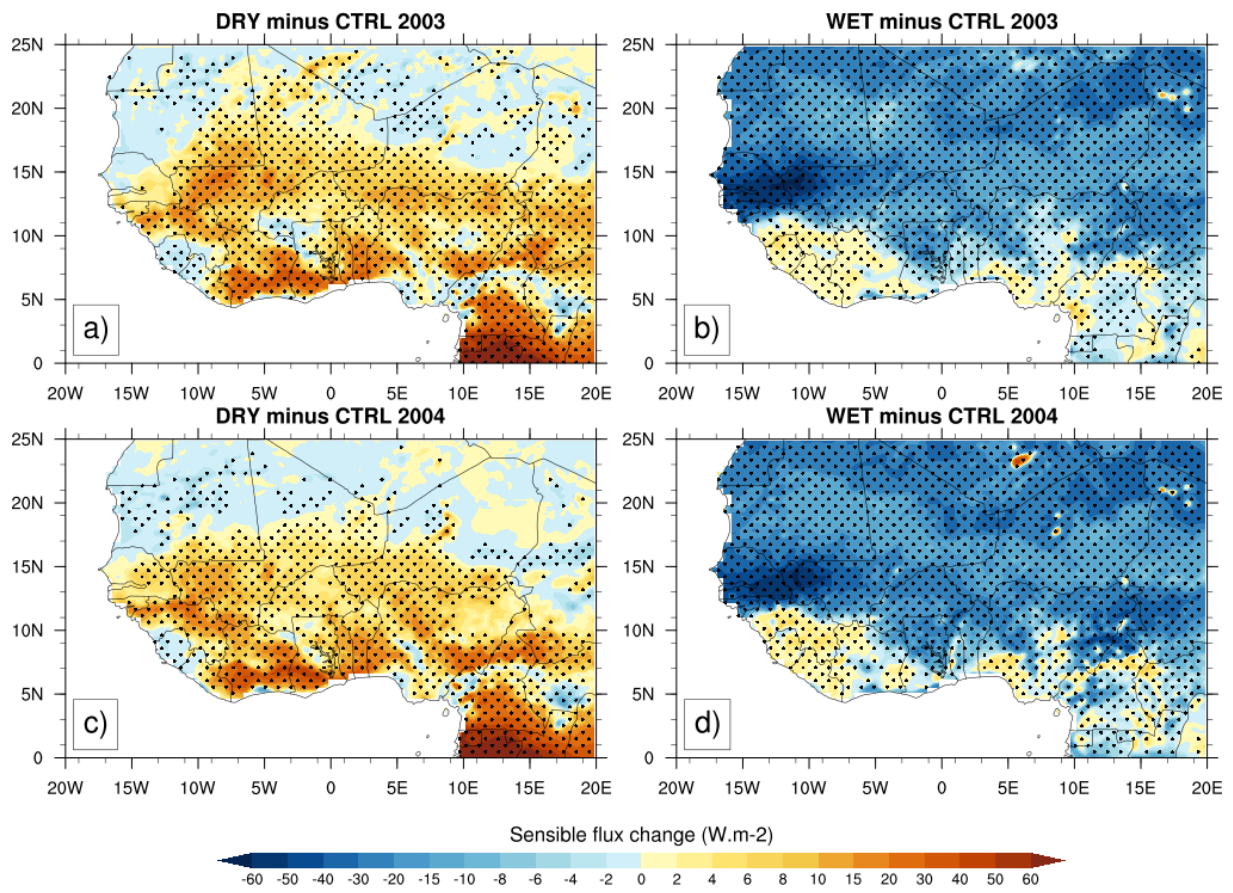
Figure 12: Changes in 2m-temperature (°C) for JJAS 2003 and JJAS 2004, from dry (resp. a and c) and wet (resp. b and d) experiments with respect to their corresponding control experiment, the dotted area shows differences that are statistically significant at 0.05 level.



950
 951
 952 **Figure 13:** PDF distributions (%) of mean temperature changes in JJAS 2003 and JJAS 2004,
 953 over (a) central Sahel , (b) West Sahel, (c) Guinea and (d) West Africa derived from dry (ΔDC)
 954 and wet (ΔWC) experiments compared to their corresponding control experiment.

955
 956
 957
 958
 959
 960
 961

962



963

964

965 **Figure 14:** Same as Fig.11 but for sensible heat fluxes (in $W.m^{-2}$).

966

967

968

969

970

971

972

973

974

975

976

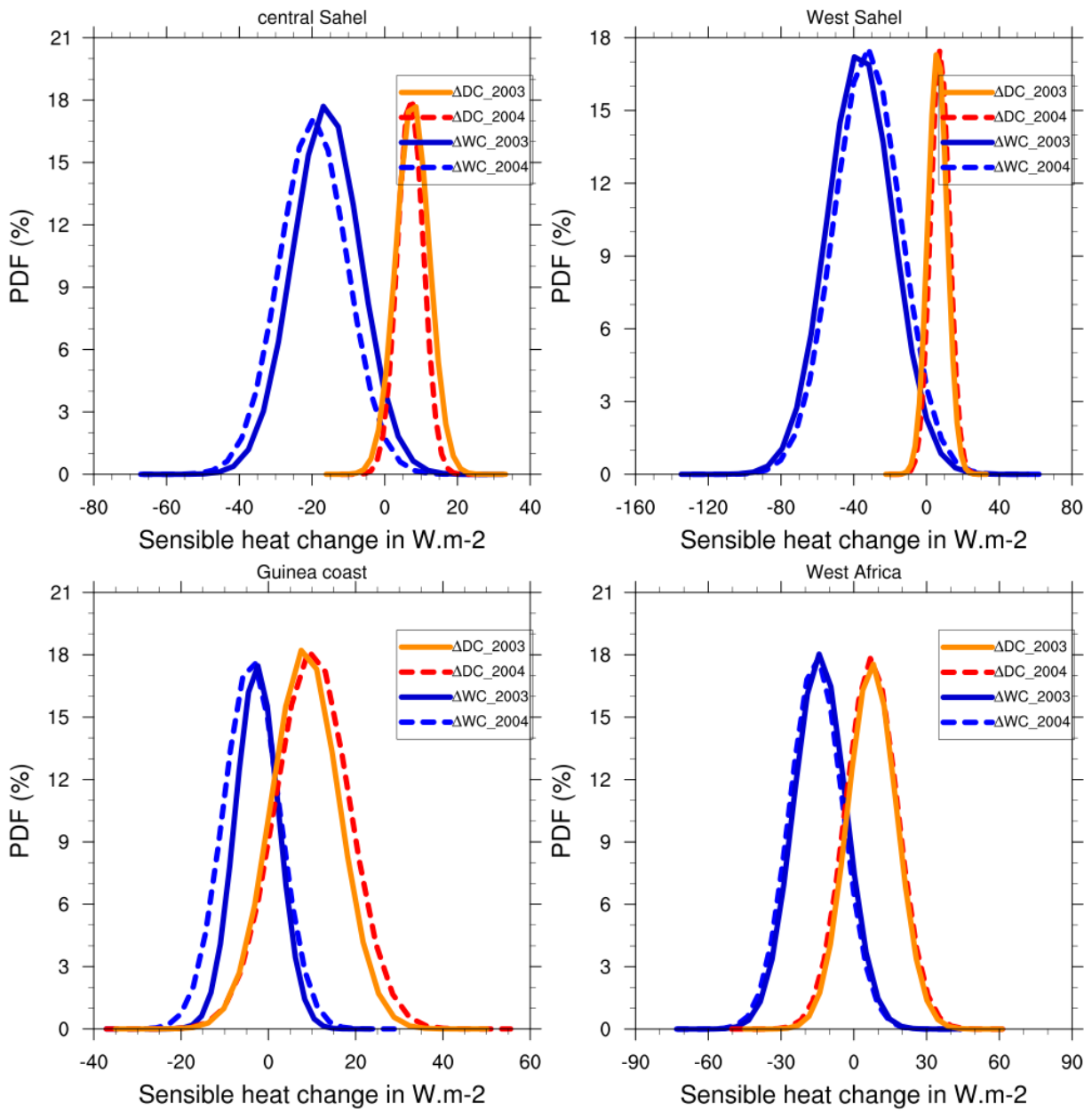
977

978

979

980

981



982

983

984 **Figure 15:** Same as Fig.12 but for sensible heat fluxes (in $W.m^{-2}$).

985

986

987

988

989

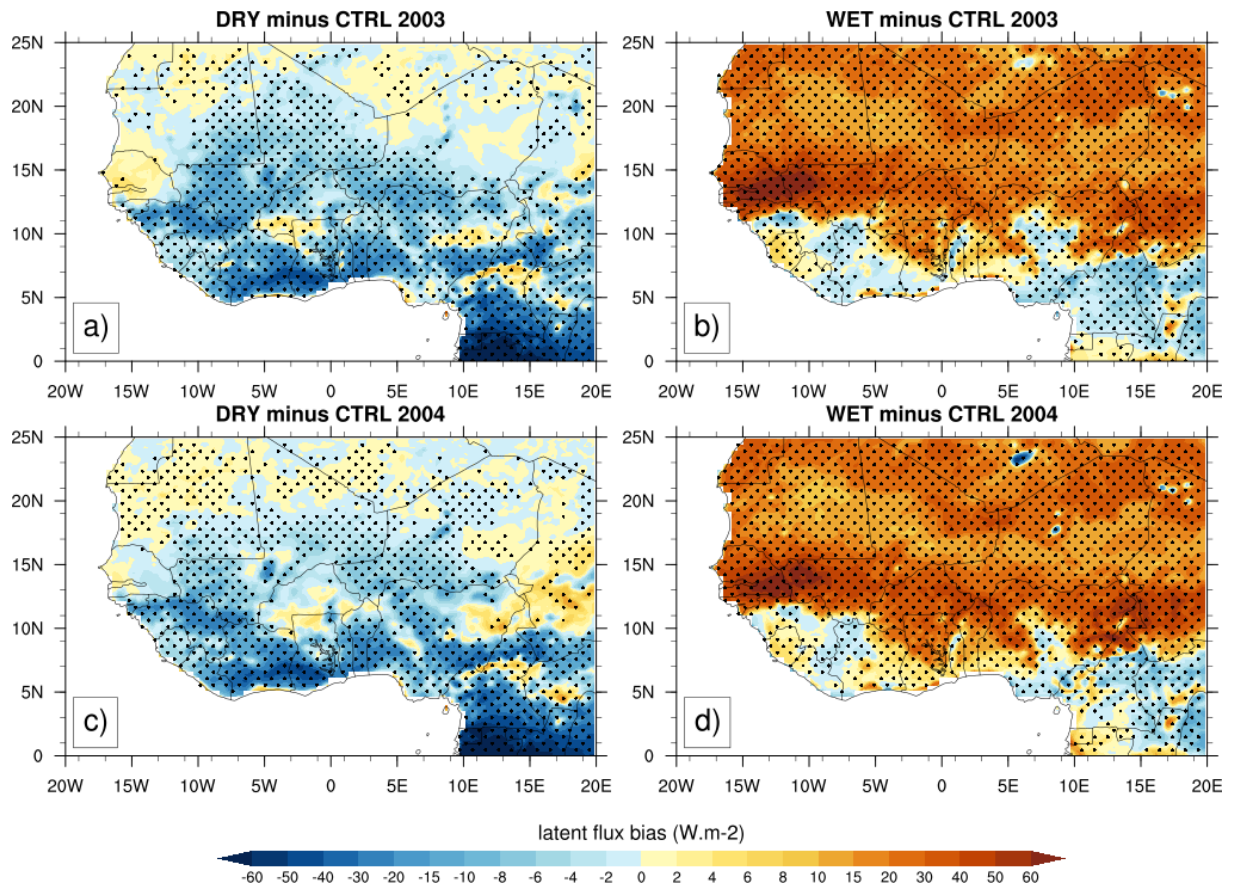
990

991

992

993

994



995

996

997 **Figure 16:** Same as Fig.11 but for latent heat fluxes (in $W.m^{-2}$).

998

999

1000

1001

1002

1003

1004

1005

1006

1007

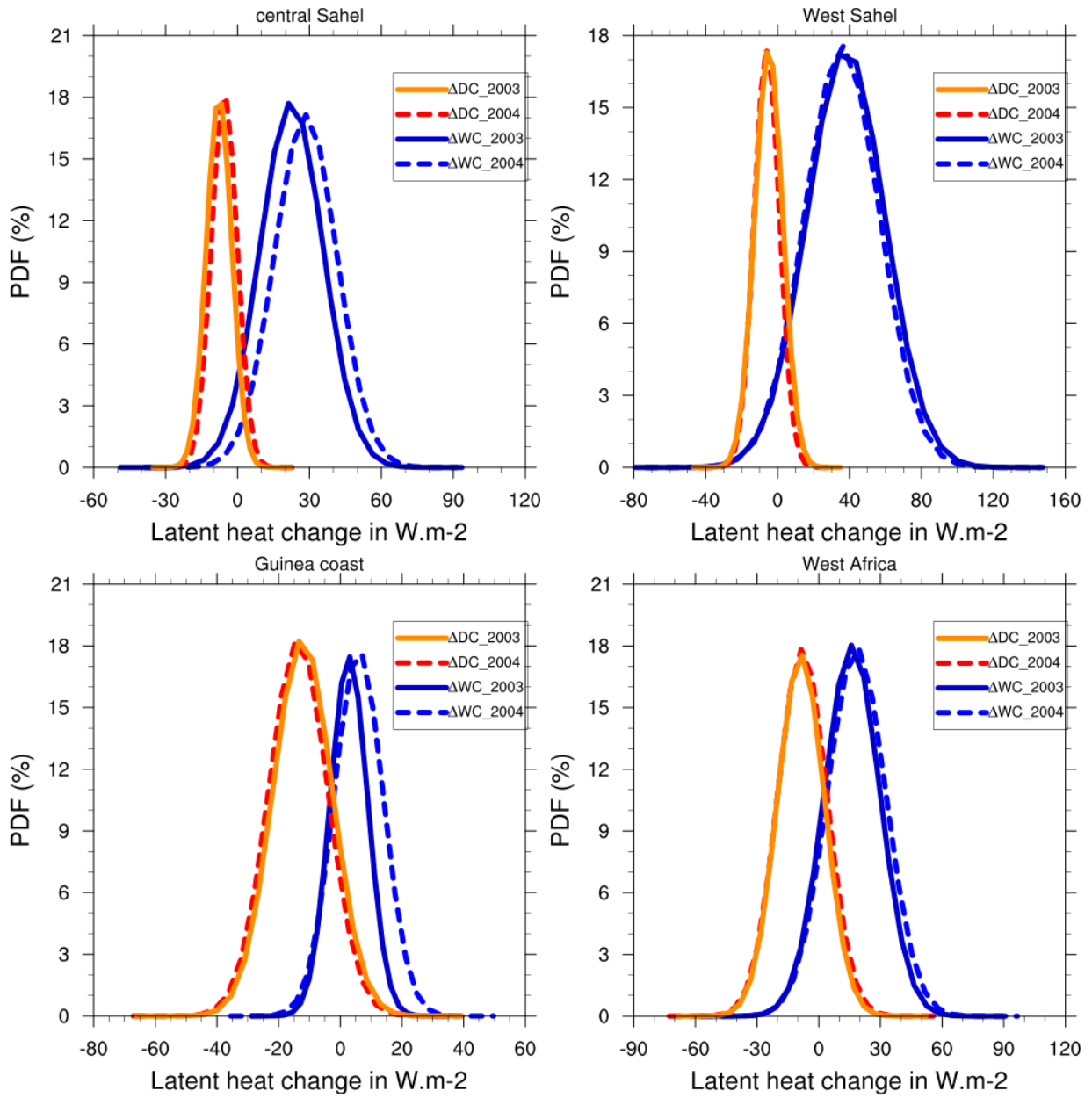
1008

1009

1010

1011

1012



1013

1014

1015

1016 **Figure 17:** Same as Fig.12 but for latent heat fluxes (in $W.m^{-2}$).

1017

1018

1019

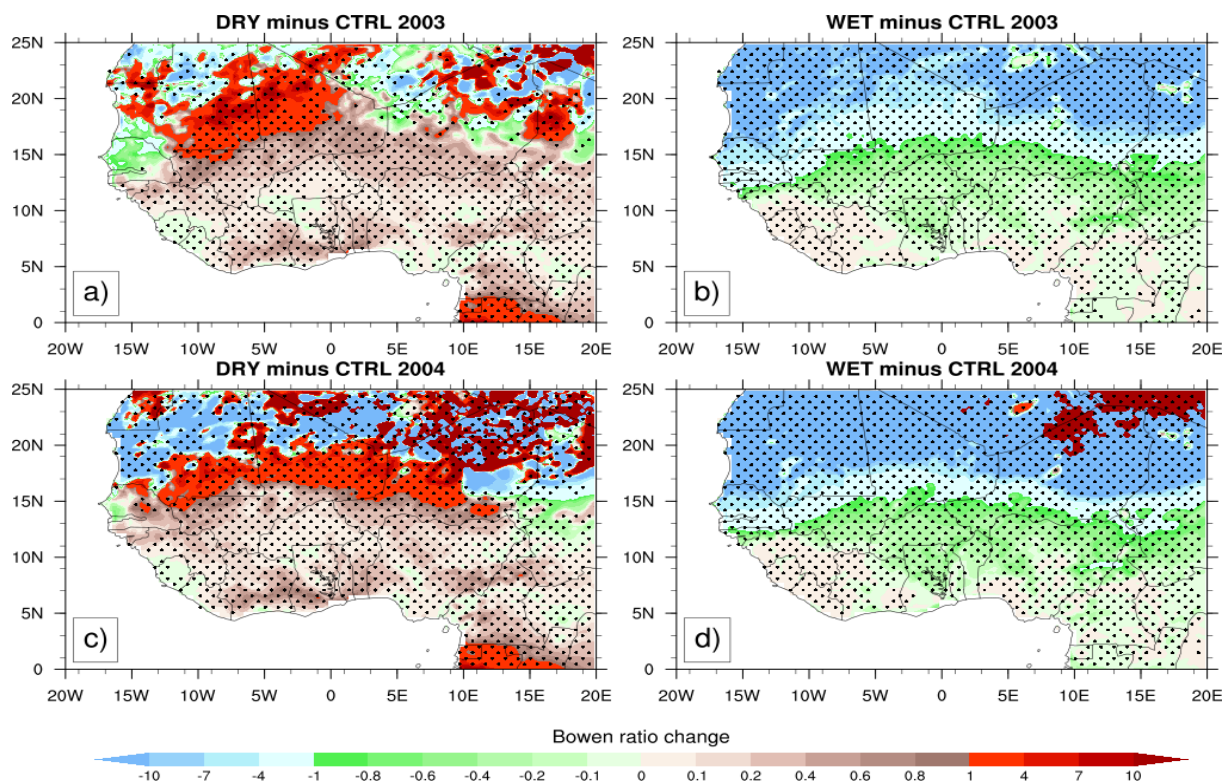
1020

1021

1022

1023

1024



1025

1026

1027 **Figure 18:** Same as Fig.11 but for Bowen ratio.

1028

1029

1030

1031

1032

1033

1034

1035

1036

1037

1038

1039

1040

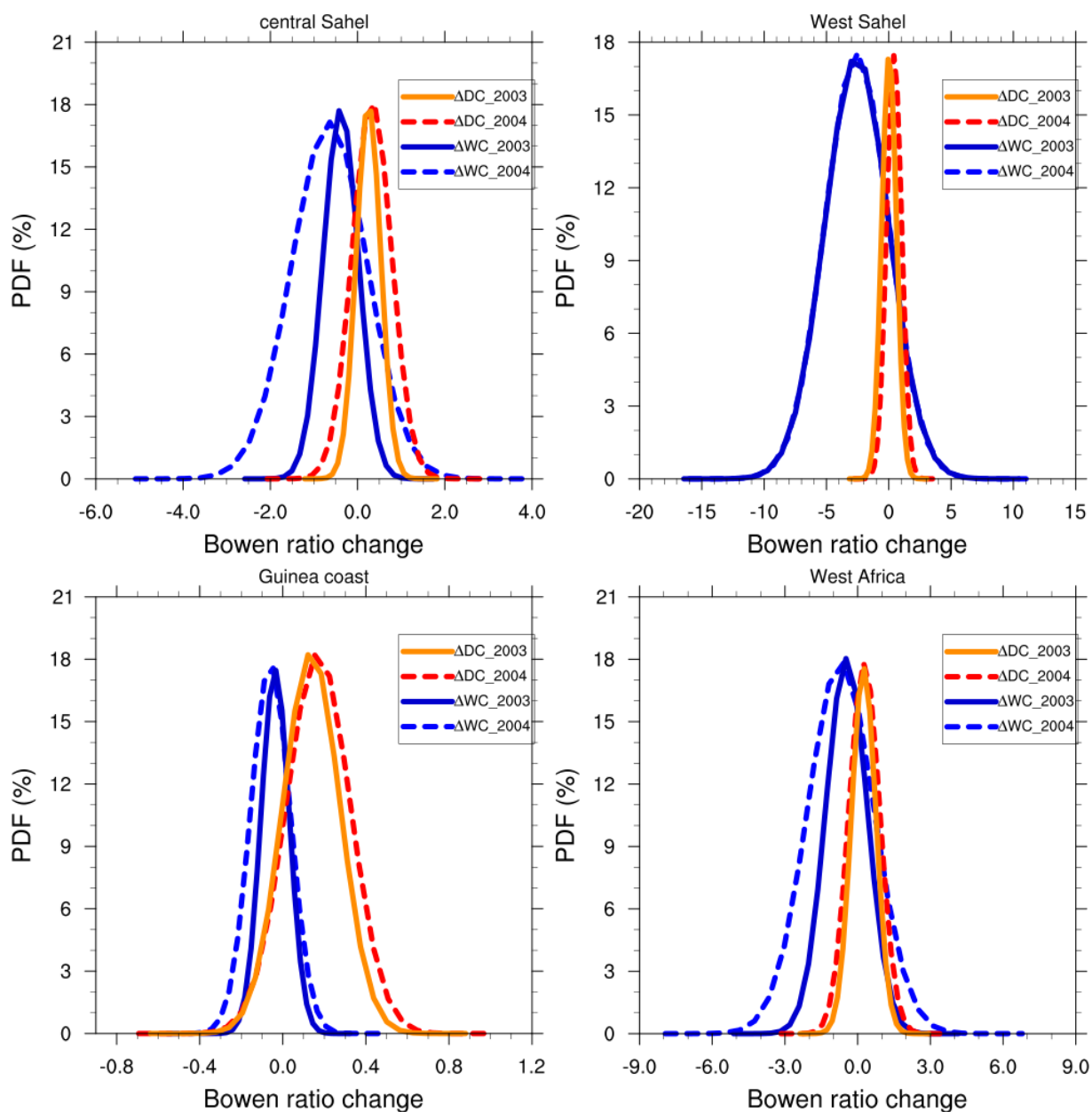
1041

1042

1043

1044

1045



1046

1047

1048 **Figure 19:** Same as Fig.12 but for Bowen ratio.

1049

1050

1051

1052

1053

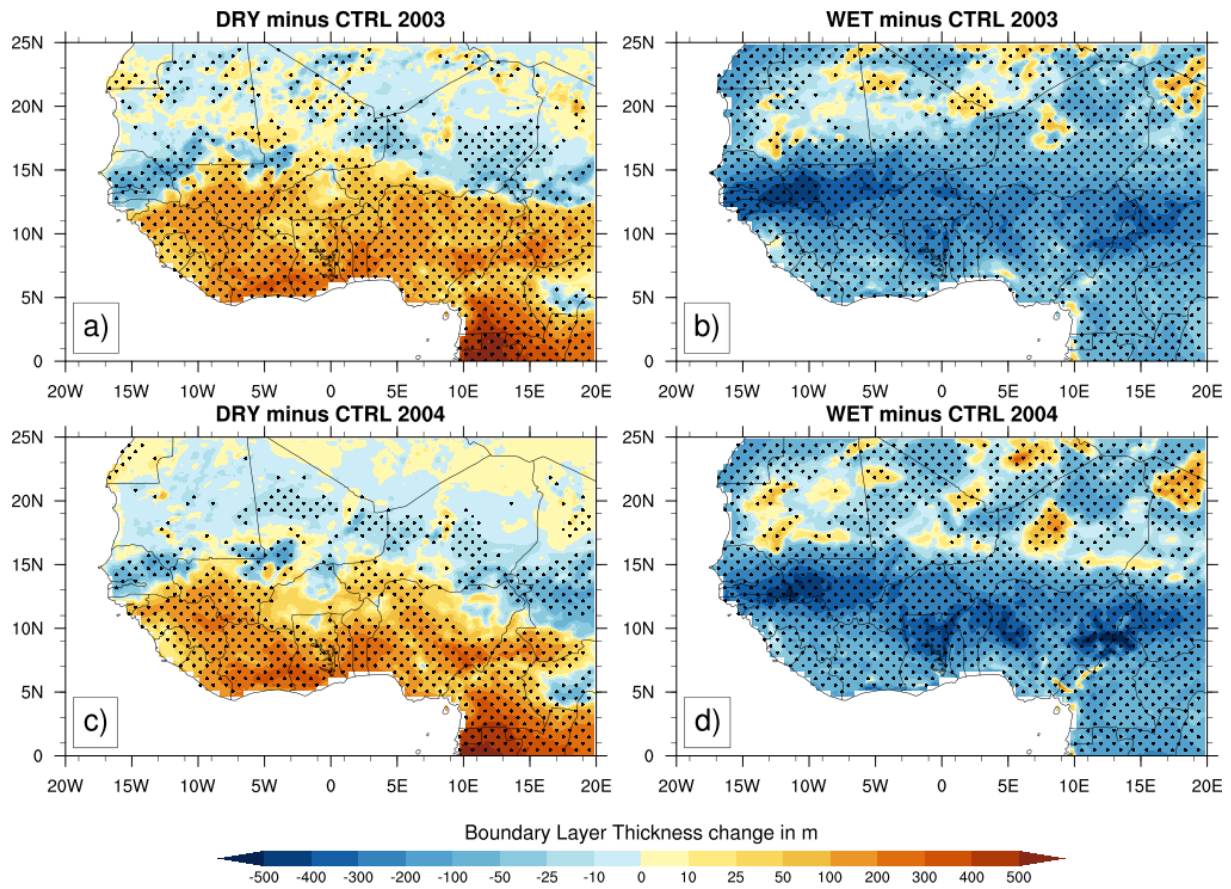
1054

1055

1056

1057

1058



1059

1060

1061 **Figure 20:** Same as Fig.11 but for the change of the height of the planetary boundary layer (in m).

1062

1063

1064

1065

1066

1067

1068

1069

1070

1071

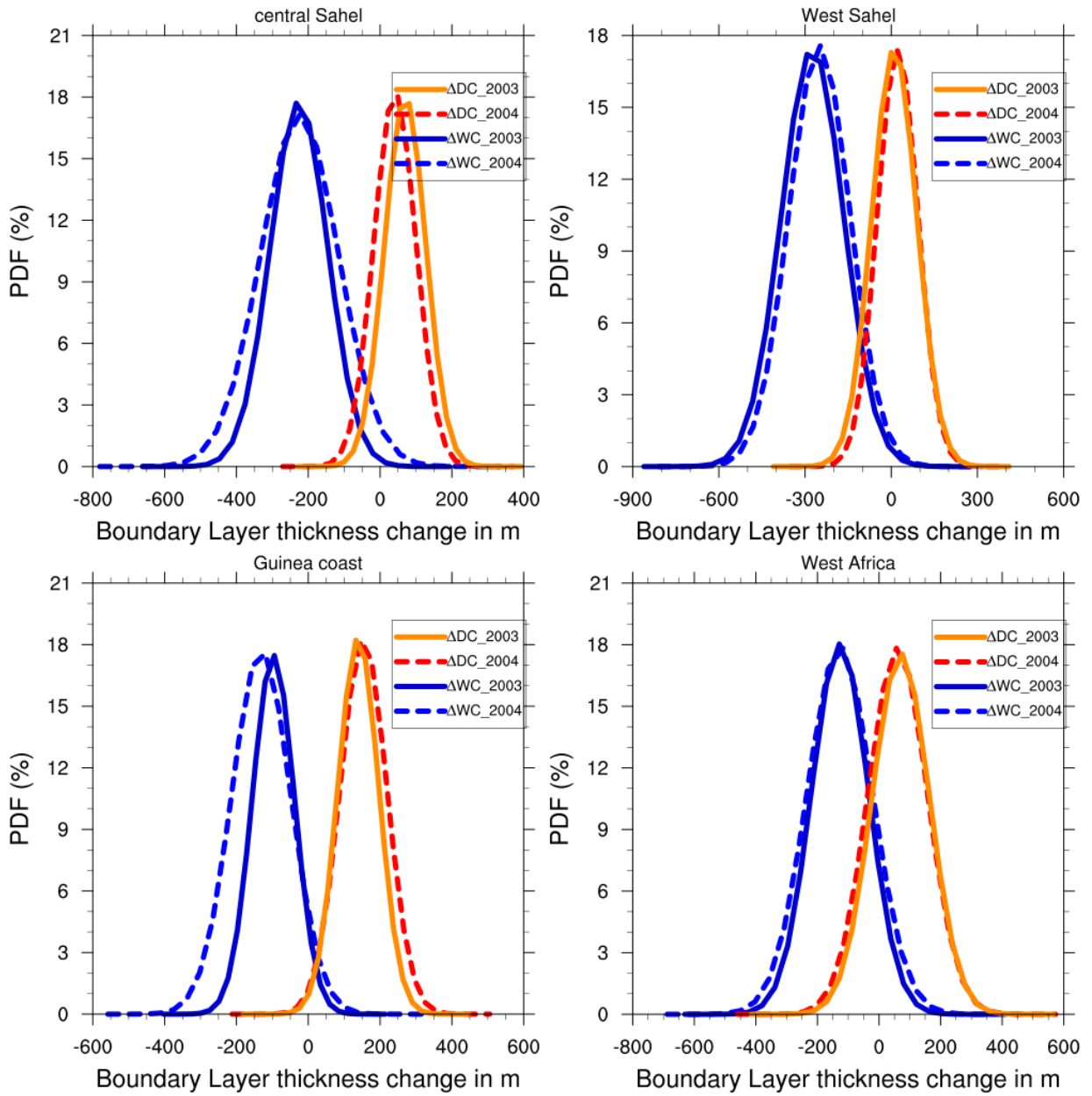
1072

1073

1074

1075

1076



1077

1078

1079 **Figure 21:** Same as Fig.12 but for the height of the planetary boundary layer (in m).

1080

1081

1082

1083

1084

1085

1086